Wageningen University

Soil Geography and Landscape

MSc Thesis Report

Testing the Meuse terrace chronology in northern Limburg using Optically Stimulated Luminescence dating

Author:
Wiebe Harder

Supervisors:
Bart Makaske
Tony Reimann

June 16, 2016

Summary

The Meuse in northern Limburg has formed multiple terraces during the transition from the Weichselian towards the Holocene (15-10 cal ka ago). This terrace staircase has been investigated in the past. For this research the terraces were sampled with optically stimulated luminescence dating (OSL). Twelve samples were taken along a 6 km long transect perpendicular to the Meuse. The samples were analysed with OSL using the Single-Aliquot Regenerative dose procedure as a proxy for single grain measurements to deal with potential partial bleaching. The minimum age model was used to derive the palaeo dose. The ages obtained were used to evaluate existing theories concerning the fluvial behavior of the Meuse.

The Meuse responded to the cold-to-warm transition of the Pleniglacial to the Bølling/Allerød interstadial with a phase of incision. The second incision phase was placed around the Younger Dryas. It is not clear whether the incision took place at the warm-to-cold (Allerød-Younger Dryas) transition or at the cold-to-warm (Younger Dryas-Holocene) transition.

There are some differences between this OSL based concept and the existing work by Tebbens et al. (1999). However, the OSL chronology is in line with the general theory concerning fluvial response to climatic reversal, creating phases of fluvial instability, causing a river to incise.

The interpretation of the OSL age of the terraces did have some difficulties. The ages obtained form the terraces did not have to represent the time of flood plain abandonment and hence the formation of the terrace. On top of the terraces there is younger sediment originating from floods of the younger terrace level: post flood plain abandonment. Following research can focus on the extend of the sedimentation and its effect on the OSL sampling and dating of the terraces. Another aspect than may require additional research is the second incision phase.

Contents

Chapter 1

Introduction

1.1 Problem description

In the second half of the previous century a lot of research has been conducted on the river Meuse. One of the aspects of these studies was to come up with a theory that describes the reaction of the fluvial system to climatic changes (Vandenberghe, 1993; Kasse, 1996). This fluvial reaction is recorded in terraces. The terraces along the Meuse in northern Limburg were formed by changes in sedimentation and erosion caused by climatic changes during the Late Weichselian and at the Weichselian-Holocene transition. Multiple attempts to identify and date these fluvial terraces, created by the Meuse during the Late Glacial, have been executed (Kasse, 1996; Huisink, 1997; Tebbens et al., 1999). Using pollen analysis, radiocarbon dating, stratigraphical evidence and other chronological data, the terraces have been assigned to certain chronozones as defined by Mangerud et al. (1974). Consequently, several theories were developed which describe the response of the Meuse system to climatic changes during the transition of the Weichselian to the Holocene.

When using the method of radiocarbon (^{14}C) to date the terraces one should focus on the earliest organic channel-fills that were left on the floodplain (Van den Berg, 1996). This method provides only a minimum age of the terrace (Törnqvist and Dijk, 1993; Tebbens et al., 1999), because there can be a considerable time lag between the floodplain abandonment and formation of peat in the channels. The time of terrace formation is defined as the moment when the former river plain is abandoned (Vandenberghe, 2014). Besides the indirect way of dating a terrace with radiocarbon, there are some other problems when dating fluvial sediments with radiocarbon: (1) limited presence of organic material in fluvial sediments, mostly only in abandoned channels in the form of peat (Tebbens et al., 1999), (2) reworking of old carbon in many fluvial sediments (Rittenour, 2008) and (3) the hardwater effect (organic carbon may come from aquatic plants that use dissolved carbonates from old, inert sources) (Tebbens et al., 1999; Grimm et al., 2009).

Tebbens et al. (1999) created a cross-section of the Meuse terrace sequence in northern Limburg. This was based mostly on ^{14}C dates and auger hole data. However, to create this cross-section, samples for ^{14}C dating had to be collected in the river valley over a length of 35 km. Later, all these spatially scattered age data were projected in a cross-section. This spatial interpolation could be a source of errors. Huisink (1997) worked along three transects, but had problems finding organic materials on some terrace levels, leading her to interpret some terrace levels in a different way compared to Tebbens et al. (1999). With the development of Optically Stimulated Luminescence (OSL) new opportunities arise to date the terraces in this area and establish a new independent chronology.

Optically Stimulated Luminescence (OSL) provides a promising method to date fluvial terraces (Wallinga, 2002; Rittenour, 2008). The great advantage of OSL is the material required for dating, which is omnipresent in most fluvial deposits: quartz. Dating the sediment itself rather than organic channel infill is a more direct way to derive an age for a river terrace. OSL however, does have its challenges when dating fluvial sediments. Problems that may arise when dating fluvial sediments with OSL include partial bleaching (Preusser et al., 2008). Partial bleaching is the incomplete resetting of the luminescence signal by solar energy before the sediment is buried. It results in age overestimations. Attenuation of light through the water column, especially when there are many suspended particles in the water, makes it hard to reset the signal in the grains during the sediment transport (Berger, 1990). Other factors that influence the bleaching process are the transport distance, mode of transport and the water depth (Rittenour, 2008). To use OSL to derive ages for river terraces is no new practice (Colls et al., 2001). However, the time span that is under consideration here is challenging. The climatic changes during the Late Glacial act on timescales of ~1000 years, which is close to the age resolution of the OSL method used for this period (Vandenberghe et al., 2013).

As there are uncertainties in the literature about the terraces and their formation in northern Limburg, additional research is required to improve the understanding of the fluvial response of the Meuse to the changes in climate during the Weichselian-Holocene transition. This improved knowledge is useful for understanding other fluvial systems around the world and can be used in modeling of future fluvial response to the changing climate. With the development of OSL a new independent method to date the terraces is available. In this way a new chronology can be created to be compared with previous work.

1.2 Research objectives

This research focuses on the river terraces of the river Meuse formed during the Late Weichselian-Holocene climatic transition. These terraces can be found in the northern part of the province of Limburg, mainly between Boxmeer and Venlo. This study zooms in on the area between the villages of Wanssum and Broekhuizen. Here all the terraces of the mentioned time frame have been identified by previous work, for example Huisink (1997) and Tebbens et al. (1999), see chapter 2 for further details.

This research tries to strengthen the understanding of the mechanisms of climatically induced river terrace formation during the Weichselian-Holocene transition. With a changing climate, understanding of the fluvial response to changes in climate is essential information. Changes in river dynamics have direct influence on the landscape and the people living close to rivers. However, how climate change will influence the river systems is still uncertain. Models are being developed to link the changes in river dynamics to predicted climate change. These models lack historical data that can be used to validate the models. Although the current climatic change is different form the change during the Weichselian-Holocene transition, it will still offer an indication of fluvial response to changes in climate. Fluvial deposits and landforms provide important archives of response to changes in climate. The chronological framework of the fluvial response of the Meuse together with palaeo climate data provides an opportunity to validate these climate change-fluvial response models.

1.2.1 Main objective

The main objective of this research is to establish an improved terrace chronology for the Late Glacial Meuse terraces in northern Limburg by an independent dating method: Optically Stimulated Luminescence (OSL). Independency of the new chronology compared to the existing ones originates from the different material used for dating. The new chronology will be compared to previous chronologies and the differences will be discussed. The differences might lead to revision of the existing climate change-fluvial response models.

1.2.2 Research questions

The research questions can be divided in two groups. The first group deals with the OSL dating of the sediments. The second group of questions is related to the interpretation of the OSL results and to the comparison with the existing theories.

The first step was to determine the OSL measurements protocol for the Meuse sediments. The general question that has to be answer is: How can the Meuse sediments be dated by means of OSL? This requires that the right treatment temperature has to be found, potential partial bleaching has to be identified, the application of age models has to be decided upon and the differences in deposition environment are also studied. These points lead to the following questions:

- Are the Meuse sediments suitable for OSL analyses?
- How well are the Meuse sediments bleached?
- Which age model is most reliable for the Meuse sediments?
- Is there a difference in the application of the minimum age model between aeolian and fluvial samples?

The final product of the main objective, the dated river terraces, can be used to answer several questions. These questions are based on concerns raised by previous researchers on the same terrace sequence (section 2.5) and on known limitations of the OSL dating technique.

The sampling design is based on a digital elevation model and maps of the terraces ages created in previous studies (Vandenberghe, 1995; Tebbens et al., 1999). This offers an opportunity to directly compare the OSL ages with the previously assign terrace ages. An interesting point are the Bølling and Allerød interstadials. They are separated by the Older Dryas cooling event (Hoek, 2001). Often this cooling event is not recognized, since it lasted only a few hundred years, which might have been too short to have an impact on the vegetation and landscape. This is why often the Bølling and Allerød interstadials are referred to as one Late Glacial interstadial. It will be interesting to see if these interstadials can be separated based on OSL dates.

This leads to the following problem: the OSL uncertainty. A common uncertainty of an OSL age is around 10% (Vandenberghe et al., 2013). With the time frame used in this study (15-10 ka ago), it can result in uncertainties of around 1000 years. This uncertainty is of the same order as the individual periods of terrace formation that are under consideration in this research, leading to potential problems when trying to identify two different terraces based solely on OSL age. Finally, the new chronological data can be used to supplement and/or adjust the existing ideas about the terraces in the study area. This leads to the following research questions:

- How do the terrace OSL ages correspond to the previously assigned terrace ages?
- Can the Bølling and Allerød terraces as identified by previous work be recognized as different terrace levels based on their OSL age?
- Is the age resolution of OSL sufficient to use this method for the time frame of 15-10 ka ago when trying to distinguish periods of 1000 years?
- Does the new chronological data urge to revise the existing theories concerning the fluvial response of the Meuse to climate changes during the Late Weichselian-Holocene transition?

1.3 Outline

This report starts with an overview (chapter 2) containing information that is essential in answering the research questions. A short description of the study area is given, followed by a summary of processes that play a role in terrace formation. There is also a description of the climate during the transition form the Weichselian to the Holocene and two theories of how the Meuse reacted to these climate changes are given. In chapter 3 the methods of the creation of the cross-section will be described, followed by chapter 4 that contains the resulting cross-section. Chapter 5 continues with the methods, describing the OSL sampling and measurements. Chapter 6 presents the OSL results. The discussion (chapter 7) focuses on the OSL results and their interpretation. At the end the conclusions (chapter 8) and the recommendations (chapter 9) are given.

Chapter 2

Background information

This chapter provides background information concerning this thesis. First, the Meuse catchment and study area will be described briefly. Next, the processes and influencing factors of fluvial terrace formation are discussed. Following this, a short summary of the climate during the Late Glacial in northwestern Europe is given. Finally, an overview of existing theories about the formation of the Meuse river terraces in northern Limburg is given.

2.1 Meuse

The Meuse is a rain-fed river. It has a catchment of 33000 km^2. The river has its source in northern France, flows through Belgium and finally enters the Netherlands in the south of Limburg. The river debouches in the North Sea (figure 2.1). In Belgium the Meuse flows through the Ardennes. This is a relatively high area with a long-term tectonic uplift. This causes the Meuse to erode in this part of the catchment, creating a sediment supply for downstream regions (Huisink, 1998). There is little reason to doubt the assumption that the catchment area has changed much in size since the Weichselien. In Limburg and northern parts of Belgium the Meuse crosses the faults of the Roer Valley rift system (see chapter2.3.1).

2.2 Study area

The area of interest is located in the lower reach of the Meuse River system, in the Netherlands between the towns of Boxmeer in the north and Venlo in the south (figure 2.1). Along this stretch of the river multiple terraces levels have been recognized. This terrace sequence is studied in this thesis. River terraces can be divided into different categories according to Bull (1991). The Meuse terraces in this area can be regarded as fill-cut terraces. This type of terrace is formed by valley aggradation (during the Pleniglacial in this case (Tebbens et al., 1999)) and subsequent downcutting of the channel and redeposition of the previously accumulated sediments. Erosion is still the dominant process in this part of the catchment. With this incision former floodplains are abandoned and a new terrace level is formed. In this way paired terraces are formed on both sides along the river (Kasse, 1996; Huisink, 1997). However, the terraces on the eastern bank are mostly covered under aeolian deposits. Large parabolic dunes are found there. Heavy mineral analysis showed that the sediments of these dunes originate from the bed of the Meuse (Huisink, 1997). In the area between Venlo and Boxmeer a smaller area has been studied and dated with OSL in this study. This area around Broekhuizervorst is interesting because here all terraces that have been identified in previous studies seem to be present along a transect (chapter 3.1).

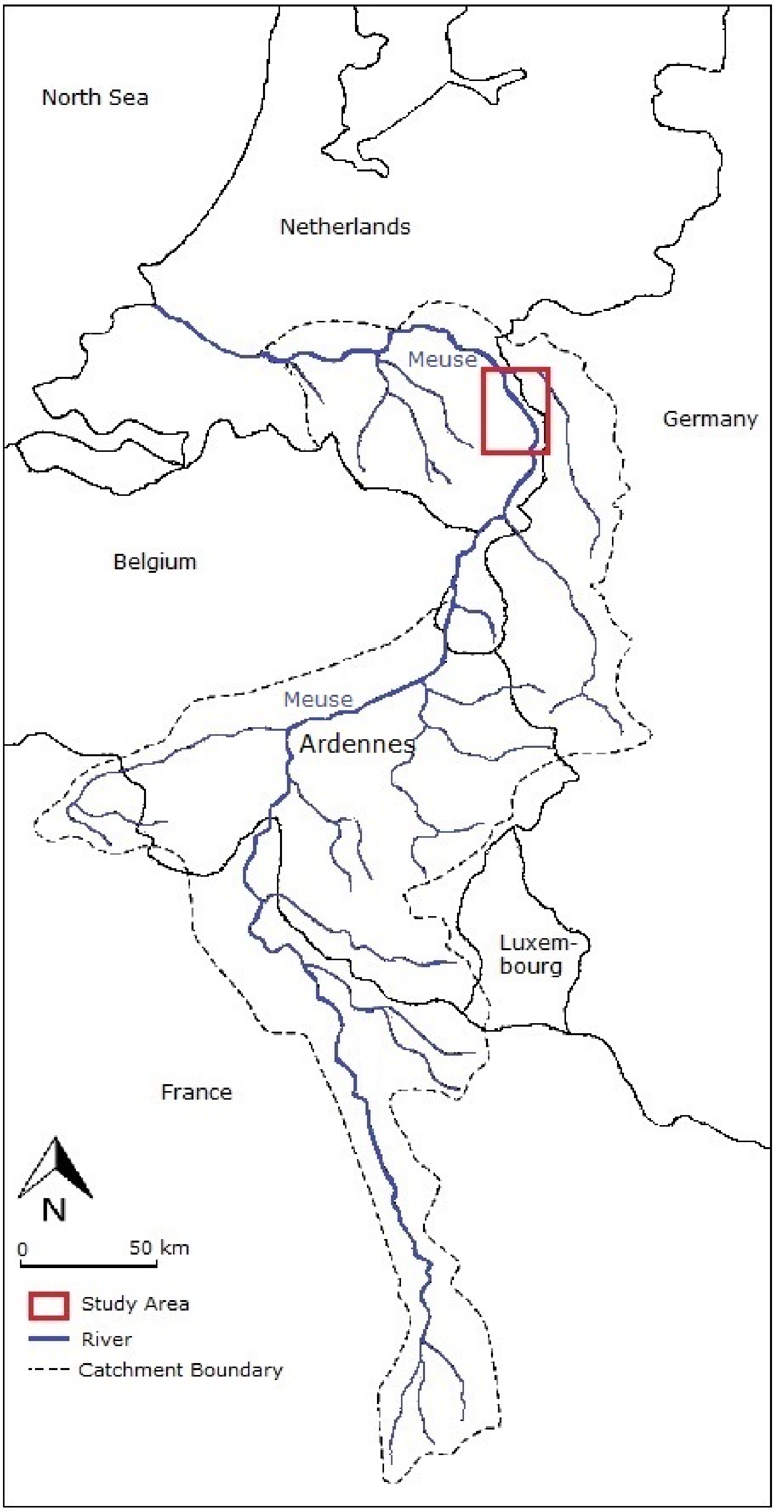

Figure 2.1: Map showing the current catchment of the Meuse. The red square indicates the study area.

2.3 Terrace formation

River systems are sensitive to tectonics, sea level and climate changes at different time-scales (Gibbard et al., 1988; Kasse, 1997; Tebbens et al., 1999). These factors influence discharge (distribution), sediment availability and the base level of the river system. In turn these variables influence the morphology of the river and whether there will be erosion or aggradation of sediments in the system. Below, each factor and the effect it has had on river morphology in the study area according to literature is discussed briefly.

2.3.1 Tectonics

The study area is part of the Roer Valley rift system. This is an active tectonic system with multiple rising and subsiding blocks. These faults are mainly NW-SE oriented (figure 2.2). During the Quaternary the system had several periods of activity (Houtgast and Van Balen, 2000). For these periods rates of up to 80 mm/ka uplift/subsidence were reported for the Roer Valley graben (Houtgast and Van Balen, 2000). The Meuse crosses multiple of these blocks: the Roer Valley graben, the Peel horst and the Venlo block (figure 2.2). The study area is located on the Venlo block. The influence of the subsiding Venlo block on the fluvial activity of the Meuse has been investigated by Huisink (1998). The main conclusion is that the changes in steepness of the terrace slopes, caused by tectonics, did not influence the Meuse river morphology (braided, meandering etc.) during the Late Glacial. Effects of the tectonics might be expressed in locally deeper incision of channels. When looking at the rates reported by Houtgast and Van Balen (2000), it can be concluded that the uplift and subsidence rates reported there are of minor influence on the rather short periods of terrace formation under consideration here.

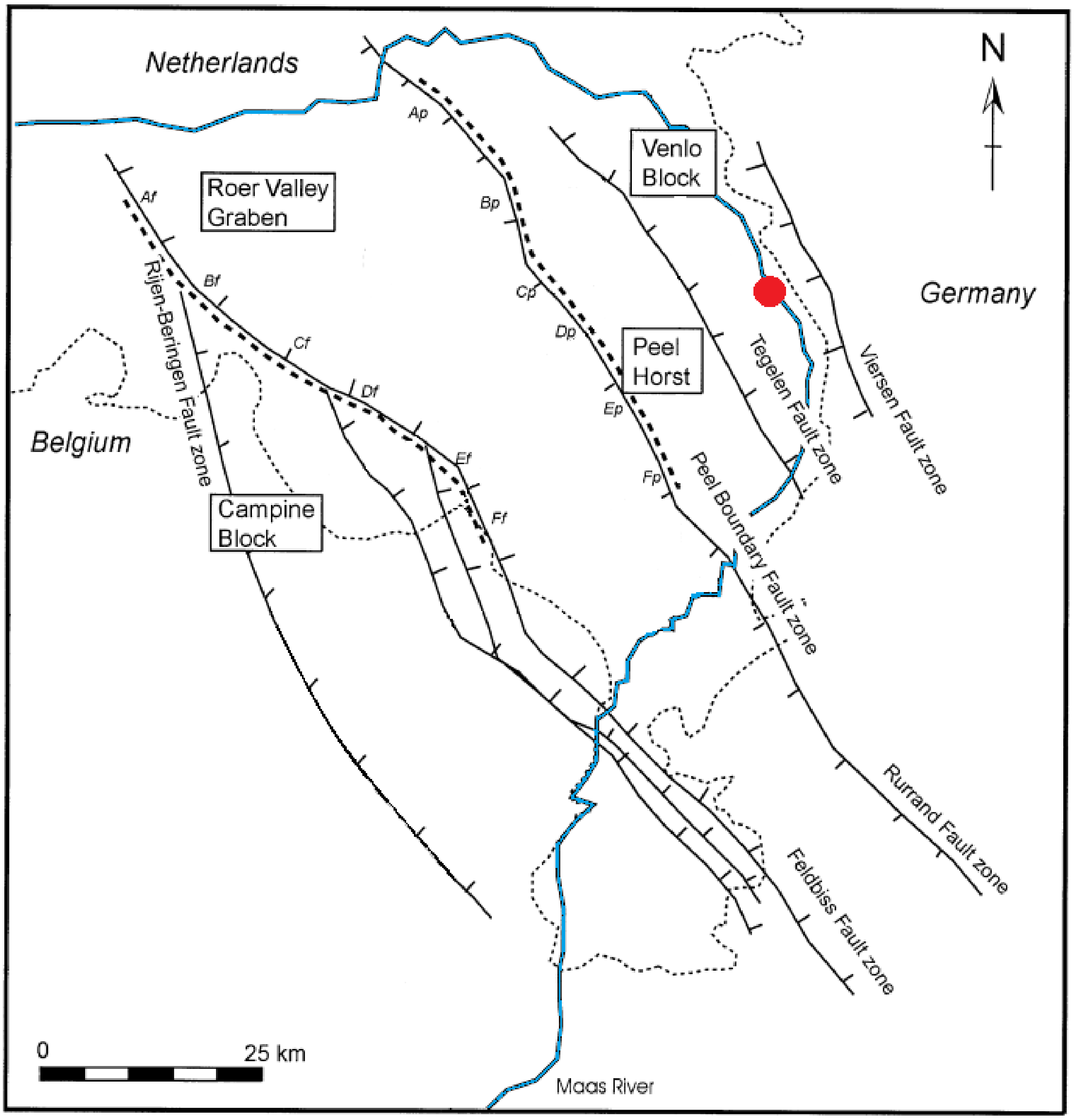

Figure 2.2: Map showing the Roer Valley systems and its faults (adapted from Houtgast and Van Balen (2000)). The red dot represents the study area.

2.3.2 Sea level

As mentioned, river behavior is also influenced by base level changes (Schumm, 1993). For most rivers the base level is the sea or a lake level. The base level of the Meuse is and has been the North Sea. During glacials the North Sea level drops drastically, meaning that the base level of the Meuse also drops. Van den Berg (1996) mentions that the influence of the base level on a river system decreases in the upstream direction. Beyond the basin's terrace crossing the effects of changing base level are negligible compared to climate and tectonic influences. Currently the terrace crossing of the Meuse is located close to Nijmegen. With dropping North Sea levels, the terrace crossing will move more toward the sea. This means that the study is and has been upstream of the terrace crossing, implying that changing base level has had minor influence on the terrace formation in the study area.

2.3.3 Climate

The response of the river to climate (change) is expressed in the river dynamics, erosion and sedimentation, which are influenced by river discharge and the sediment load. Climate can influence these two aspects in many different ways. Temperature and precipitation are the key climatic parameters in determining whether erosion or sedimentation will occur (Vandenberghe, 2003). Of course, temperature and precipitation are important direct drivers for the discharge regime of a river (Vandenberghe, 2002). Temperature and precipitation also have indirect influence on a river system. One of the most important actors influenced indirectly is vegetation. Vegetation cover controls the surface erosion, mass wasting or aeolian activity and influences the water balance of the river catchment by evapotranspiration (Kasse et al., 2003; Vandenberghe, 2003). The simple relation is that with a discontinuous or absent vegetation cover, more sediment will be available for the river to transport (Tebbens et al., 1999). As stated by Vandenberghe (1993, 1995) and Mol et al. (2000) rivers mainly act on the cold-warm and warm-cold transitions, because this is when the largest changes in vegetation occur. An other climate-driven factor is the presence or absence of permafrost (Vandenberghe, 2002). It affects the discharge distribution of a river system in time (Mol et al., 2000). Frozen ground reduces soil permeability drastically, enhancing surface runoff and concentrating the runoff in a short period during the melt season. Another effect of the frozen ground is the lack of groundwater flow resulting in low base flow of the rivers, allowing them to dry up (Woo and Winter, 1993).

Whether changes in precipitation and temperature, and the following changes in vegetation and permafrost occurrence, actually force a river to react, depends on the threshold for geomorphological change of the river system (Schumm, 1979). This threshold needs to be exceeded before any morphology changes can succeed. The duration of the climatic disturbance also has to be of considerable length, since there is a lag time in the response of vegetation to changing climate (Tebbens et al., 1999). This lag time is very important in the fluvial response of the Meuse. When a climatic change is too short, no clear response in vegetation and in river morphology is observed (Bull, 1991; Kasse, 1996).

2.4 Climate during the termination of the last glacial period

For the area that is under consideration here, there seems to be an agreement that climate is the driving factor behind the formation of the terrace sequence (Huisink, 1997; Vandenberghe, 2014). This will be used as the starting point of view for this thesis. The climate during the transition from the Weichselian to the Late Glacial and finally to the Holocene will be described in this section. An overview can be found in figure 2.3. After this palaeo climate information, a section describing the existing theories about how the Meuse responded to this climate changes in the past and how this influenced the terraces will be given (section 2.5).

2.4.1 Late Pleniglacial

The Late Pleniglacial (22.0-15.7 ka ago, MOI stage 2) is mainly characterized by the retreat of the ice sheet that covered northern Europe and part of Britain (Huijzer and Vandenberghe, 1998). During the first half of this period the mean annual temperature was probably around -4 °C, as indicated by the presence of ice-wedge casts. Summer temperature would have been around 8 to 10 °C. Gradual warming occurred in the second part of this period (Huijzer and Vandenberghe, 1998). The cold climate resulted in very sparse vegetation (Walker, 1995; Hoek, 1997). Lack of vegetation and arid conditions enhanced aeolian activity during the Late Pleniglacial (Kasse, 1997; Hoek, 2000). Loess and cover sands were deposited all over northwestern Europe.

2.4.2 Bølling

The first interstadial of the Late Glacial spans from 15.7 to 14.2 ka ago. There is a distinct temperature rise with respect to the Pleniglacial with summer temperatures ranging from 16 to 18 °C (Bohncke, 1993; Walker, 1995). Effective precipitation increased (Bohncke, 1993) and in time vegetation responded to the increase in temperature and precipitation (Walker et al., 1994), leading to an open boreal forest (Bohncke, 1993; Walker, 1995; Hoek, 2000). The more humid conditions and more continuous vegetation cover resulted in cessation of aeolian processes and favored soil formation (Bohncke, 1993).

2.4.3 Older Dryas

The Older Dryas (14.2-13.8 ka ago) is not recognized in every geological record (Bohncke, 1993). When found, it is often reflected in pollen data by a reduction in trees and an increase in open vegetation, resulting in more disturbed and degrading soils (Walker, 1995). This change in vegetation is often attributed to a drop in winter temperatures and a decrease in precipitation (Kasse, 1996; Walker, 1995). Annual temperature did not reach below -1 °C since no periglacial structures have been found, whereas mean summer temperatures should have ranged between 14 to 16 °C (Bohncke, 1993). Evidence for renewed aeolian activity and the formation of river dunes is found in the Netherlands and Belgium (Bohncke, 1993; Walker et al., 1994).

2.4.4 Allerød

The Allerød is the second Late Glacial interstadial, lasting from 13.8 to 12.8 ka ago. The summer temperatures during the first part of the Allerød were quite similar to those during the Bølling, but winter temperatures were slightly higher (Bohncke, 1993). Soils were stable (Walker et al., 1994) and there was no aeolian activity due to ample vegetation. During the second part of the Allerød (13.3-12.8 ka ago) the precipitation decreased again (Kasse, 1996). Lower temperatures during the winter resulted in more intense action of freeze-thaw cycles, promoting unstable soil conditions (Bohncke, 1993). Evidence for these changes in temperature is the advance of *Pinus* during the later part of the Allerød (Bohncke, 1993; Hoek, 2000).

2.4.5 Younger Dryas

At the transition from the Allerød to the Younger Dryas (12.8-11.8 ka ago), the climate became colder and the decline in effective precipitation that started in the second phase of the Allerød continued and most trees died (Bohncke, 1993; Hoek, 2000). The presence of ice-wedges indicates mean annual temperatures of -4 °C (Kasse, 1996), with summer temperatures around 10 °C (Bohncke, 1993). The decline in trees (*Pinus*) is probably the result of the dropping summer temperatures and an decrease in precipitation (Bohncke, 1993). During the second part of the Younger Dryas (12.3 -11.8 ka ago) river activity became minimal during winter and the dry riverbed acted as a source area for aeolian sediments (Walker et al., 1994). These sediments were blown towards the vegetated valley sides and formed parabolic dunes (Bohncke, 1993; Kasse, 1996). Parabolic dunes are still clearly visible on the eastern bank of the Meuse. At the end of the Younger Dryas most forest was replaced by shrub vegetation (Bohncke, 1993; Hoek, 2000).

2.4.6 Holocene

The beginning of the Holocene (dated around 12 ka ago, but some uncertainty due to a carbon plateau (Walker et al., 1994)) is characterized by a steep increase in temperature. Summer temperatures were restored to those approximately equal of the previous interstadial: 15 to 17 °C. During the first ~1000 years of the Holocene (the Preboreal) there were still some minor temperature fluctuations (Walker et al., 1994). Increasing effective precipitation enhanced vegetation growth and within 500 year the tundra vegetation was replaced by woodland (Walker, 1995). This resulted in ceasing of aeolian activity and less sediment input in lakes and rivers (Bohncke, 1993).

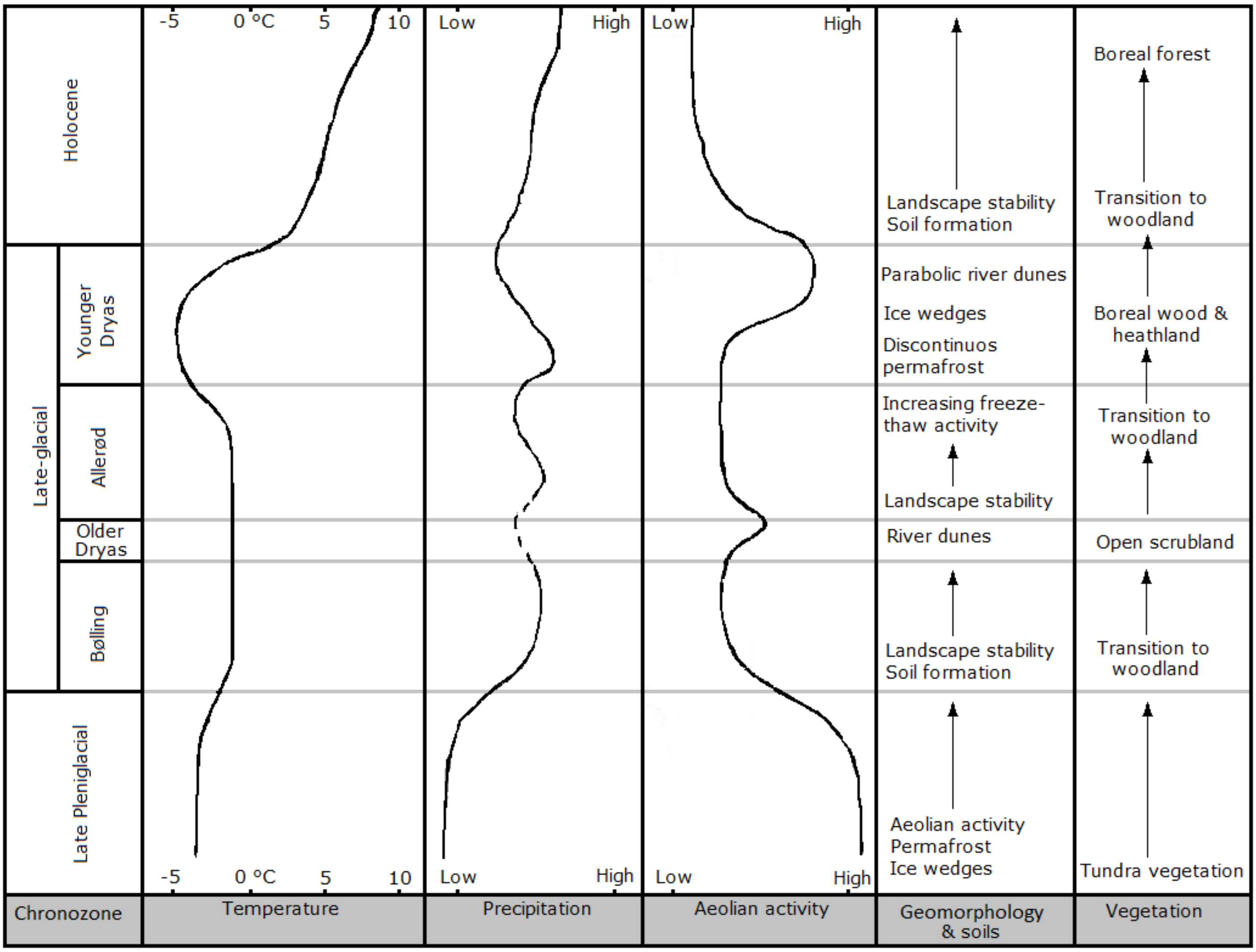

Figure 2.3: Summary of the Late Glacial climate.

2.5 Existing theories

2.5.1 Pleniglacial

During the Pleniglacial fluvial activity probably only occurred in the valleys during spring time with high peak discharges due to melt water (Huijzer and Vandenberghe, 1998). The rivers were probably braided systems in response to these highly energetic melt water flows (Huijzer and Vandenberghe, 1998; Huisink, 1997). Aggradation of these systems together with deposition of aeolian sediments resulted in slight accumulation in the river valley. This Pleniglacial braided river system formed a wide terrace, as is distinctive for a braided system (Vandenberghe, 2008). Both Huisink (1997) and Tebbens et al. (1999) describe an aggrading braided river system during the Pleniglacial. This is the result of the sparse vegetation cover, resulting in high sediment availability.

2.5.2 Bølling

Due to the more constant river discharge and lower sediment supply to the river following the increasing vegetation cover and higher precipitation, no more aggradation took place during the Bølling. The Meuse started to incise into its former braided river floodplain. Huisink (1997) describes this as a gradual transition from the braided system towards an Allerød meandering system. According to Tebbens et al. (1999) the larger braided channels started to incise in the Pleniglacial floodplain. This resulted in a meandering system with multiple deep channels in the Bølling.

The main difference between Tebbens et al. (1999) and Huisink (1997) is the response time of the Meuse to the cold-to-warm climate transition. Tebbens et al. (1999) envisions a fast response of the Meuse while Huisink (1997) claims a slow transition from a braided towards a meandering river system.

2.5.3 Older Dryas

Tebbens et al. (1999) mentions a pause in the downcutting and in the shifting of meanders of the Bølling-Meuse during the Older Dryas, but no clear evidence is presented. Huisink (1997) does not mention the period since there are no deposits found from the Older Dryas along the Meuse. The duration of the Older Dryas is probably too short to have had a major influence on the morphology of the Meuse (Vandenberghe, 1995). The geomorphological threshold described earlier was probably not exceeded during this period.

2.5.4 Allerød

After the transitional phase during the Bølling the Meuse turned into a meandering system during the Allerød (Huisink, 1997). This system was shifting laterally and slowly eroding. Tebbens et al. (1999) expects that Meuse activity was similar to its activity during the Bølling: meandering and incising. The main difference with the Bølling is that during the Allerød the erosion took place as floodplain lowering instead of channel incision. Towards the end of the Allerød, the climate started to cool. According to Tebbens et al. (1999) the Meuse already started to adapt a more braiding pattern, while Huisink (1997) postulates that the meandering system persisted through the entire Allerød.

2.5.5 Younger Dryas

Tebbens et al. (1999) and Huisink (1997) disagree about the behavior of the Meuse during the Younger Dryas stadial. According to Tebbens et al. (1999) the Meuse continued with adapting its pattern, which already started to change during the later part of the Allerød. Due to the colder climate and disappearing vegetation the Meuse changed into an aggrading braided system once more. Huisink (1997) agrees that in the Younger Dryas the Meuse is a braided river system. However, there are some disagreements about the geomorphological processes. Huisink (1997) claims that at the start of the Younger Dryas the Meuse entered a periods of extreme incision, up to 10 meters in depth. This would have been the result of a higher but more irregular discharge regime while the vegetation was still intact. Later in the Younger Dryas sedimentation took over but was not able to fill the incisions created earlier in the Younger Dryas. Tebbens et al. (1999) did not find evidence for this extreme erosional phase.

Again there is a difference between both papers in the reaction speed of the Meuse to a climatological transition. This time there was a warm-to-cold transition. While Tebbens et al. (1999) see a gradual adaptation of a braided river system, Huisink (1997) mentions a abrupt change from a meandering system toward a dramatic incision phase and development of a braided system.

2.5.6 Holocene

In the Holocene the Meuse started to incise a little and developed a slightly meandering course (Huisink (1997); Tebbens et al. (1999)). Human influence starts to play a role during the late part of the Holocene, increasing the sediment availability by deforestation and other agricultural activities. In the last centuries the course of the Meuse has been heavily influenced by humans. A large part of the Younger Dryas floodplain has been eroded away by the Holocene Meuse.

Chapter 3

Methods - Cross-section

Before the OSL samples could be collected, it was necessary to gain insight in the lithological situation. The first step was to identify a suitable transect for the OSL sampling in the study area. After the transect was decided upon, the next step was to create a lithological cross-section along this transect.

3.1 Transect

The major criterion for the transect was that all previously identified terraces (e.g by Huisink (1997); Tebbens et al. (1999)) are present along the transect. Additional criteria were land use, forest had the preference, and accessibly. Forest was preferred over agricultural fields due to the smaller risk of soil mixing/disturbances compared to agricultural fields. With these criteria four possible transects were planned. An exploratory field survey was conducted to choose one of the four transects as the final one. During this survey shallow augerings (up to 1.20 m) were made to get insight into the lithological conditions and to check for possible soil disturbances.

The chosen transect spans roughly 6 km and has a NE-SW orientation, perpendicular to the flow direction of the Meuse (figure 3.1). This transect was chosen because of the complete sequence of terraces and the presence of suitable sampling locations, located mainly in forests and nature areas. Another aspect that favors this transect is that it is the location of educational field practicals of Wageningen University.

3.2 Cross-section

Along the selected transect 40 augerings (figure 3.1) were carried out up to a depth of 2.5 m. The goal of the augerings was to observe differences in texture and grade of sorting of the sediments. The grain size of sand was measured in the field with a sand ruler. Based on this collected data and existing data (cross-section from Miedema et al. (1983)) a new cross-section was made. The surface elevation was derived from the AHN (Dutch National Elevation model). The purpose of the cross-section is to give a clear overview of the terraces along the transect and to be able to select suitable locations for OSL dating. Furthermore the cross-section provides a clear overview when comparing the different ages obtained from the OSL measurements.

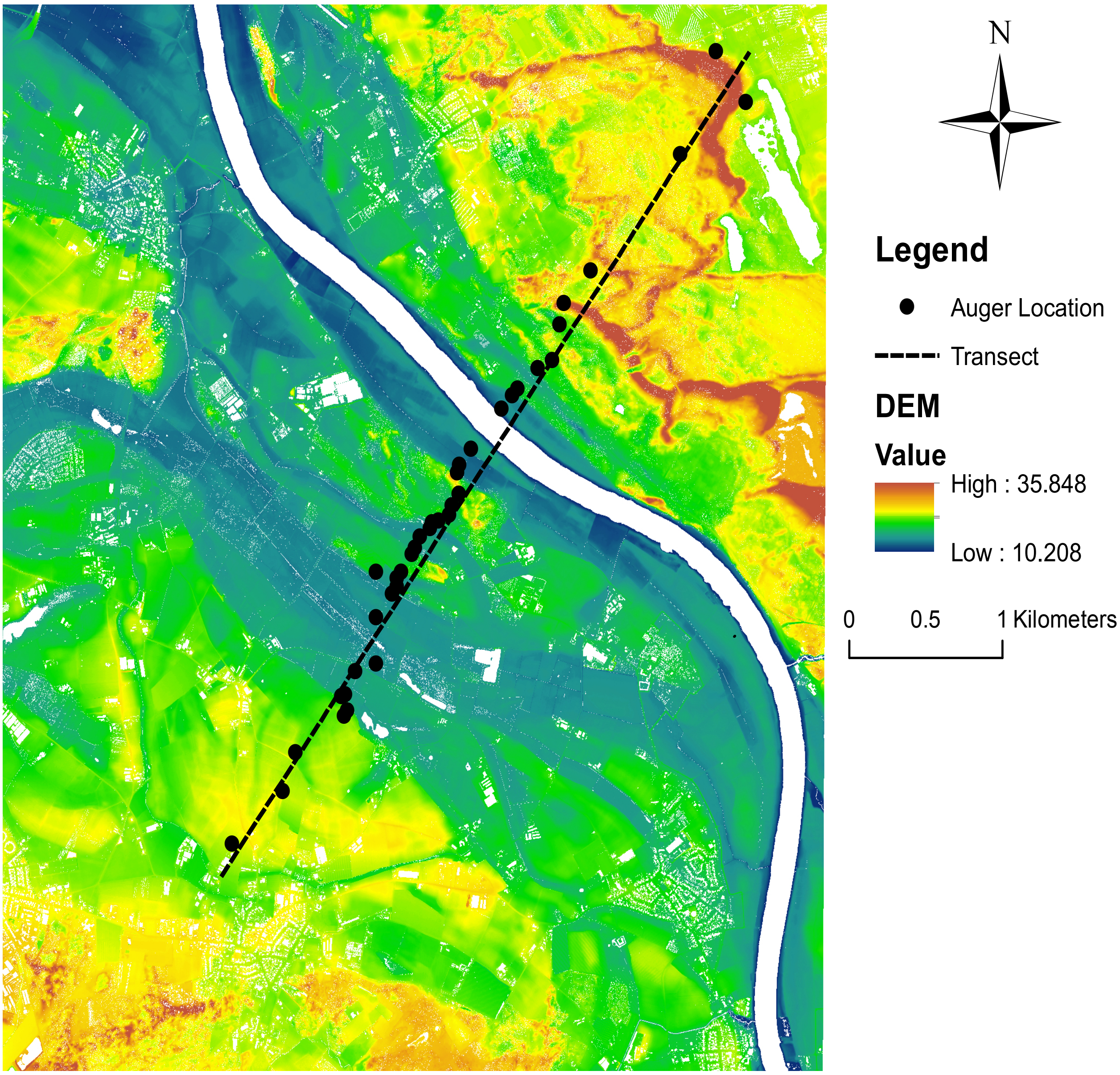

Figure 3.1: Digital elevation model of the study area and the transect with the auger locations. DEM adapted from the AHN (www.ahn.nl).

Chapter 4

Results - Cross-section

The result of the 40 augering is presented in figure 4.1. The resulting lithological cross-section will be used to design the OSL sampling design (section 5.1).

4.1 Sediment classes

There are seven different sediment classes in this study (figure 4.1). Here the main characteristics of each class will be described shortly. There are four sand classes, they will be described first. The fine sand class is generally well sorted sand with median grain size of 150-210 μm. The sand class is somewhat coarser than the fine sand class, having their median grain sizes at 210-300 μm. Coarse sand is generally more poorly sorted than the sand class. The median grain size of this class is roughly 200-420 μm, but some larger gravels can be present. It is distinguished from the sand class by its grade of sorting/presence of gravels. The last sand class is the sandy gravel. This class is characterized by its poorly sorted sediments and its high gravel content and large median grain size (>420 μm). The space between the fine sand class and the clay class is taken by the silt class. The grains are smaller than 150 μm and well sorted. The clay class consist of light and heavy class, no distinction is made in this study. The organic sediments are all part of the peat class.

4.2 Morphological structures

Three main types of morphological structures can be recognized in the cross-section (figure 4.1).

- **River terraces**: mainly sandy sediment and a fining upwards sequence. Often higher in the landscape than the channels.
- **Channels**: most abandoned now. Mainly clay and peat have filled the channels.
- **River dunes**: Consisting of sand, have a different morphology than the river terraces.

This information helps in choosing the right location to sample with OSL. This ensures that every river terrace level is dated at least once.

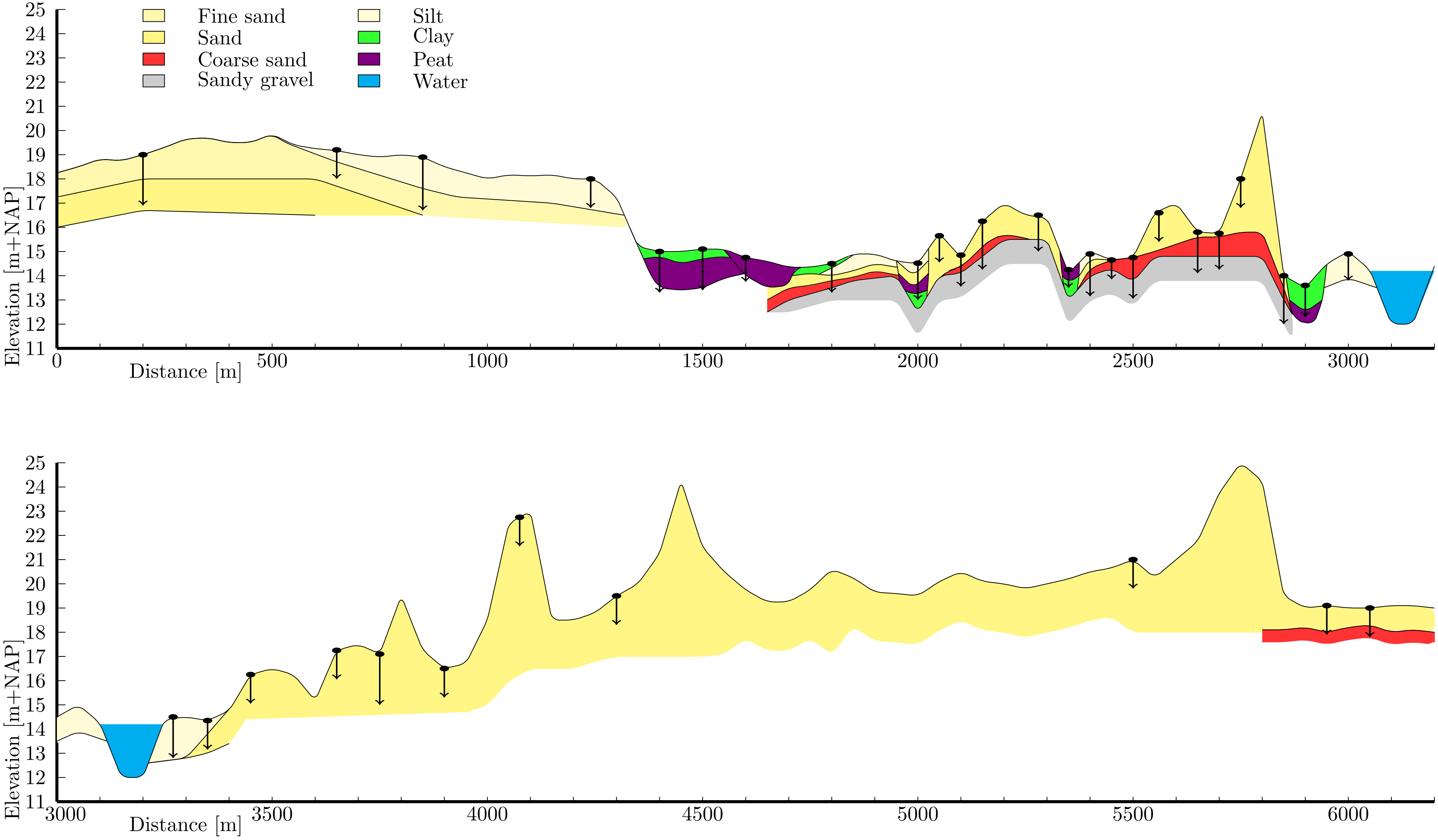

Figure 4.1: Lithological cross-section along the transect. The dots represent the auger locations and the arrows indicate the depth op the augering.

Chapter 5

Methods - Optically Stimulated Luminescence dating

After the lithological cross-section was made, the OSL sampling locations could be selected. The sampling selection and collection procedures are described first. After that the following OSL analysis in the lab is described in this chapter. Finally the application of the age models is described.

5.1 Sampling locations

The goal was to sample each terrace level that has been identified in previous studies (Huisink, 1997; Tebbens et al., 1999) at least once. The cross-section (chapter 4) was used to confirm this. This resulted in 12 locations that had to be sampled. 10 samples were taken from fluvial terraces and 2 samples were taken from the river dunes, one from each bank (east and west). In figures 5.1 and 5.2 the chosen OSL locations are shown. In table 5.1 a summary is given of the sampling locations characteristics, as well as an expected age based on literature (Tebbens et al., 1999).

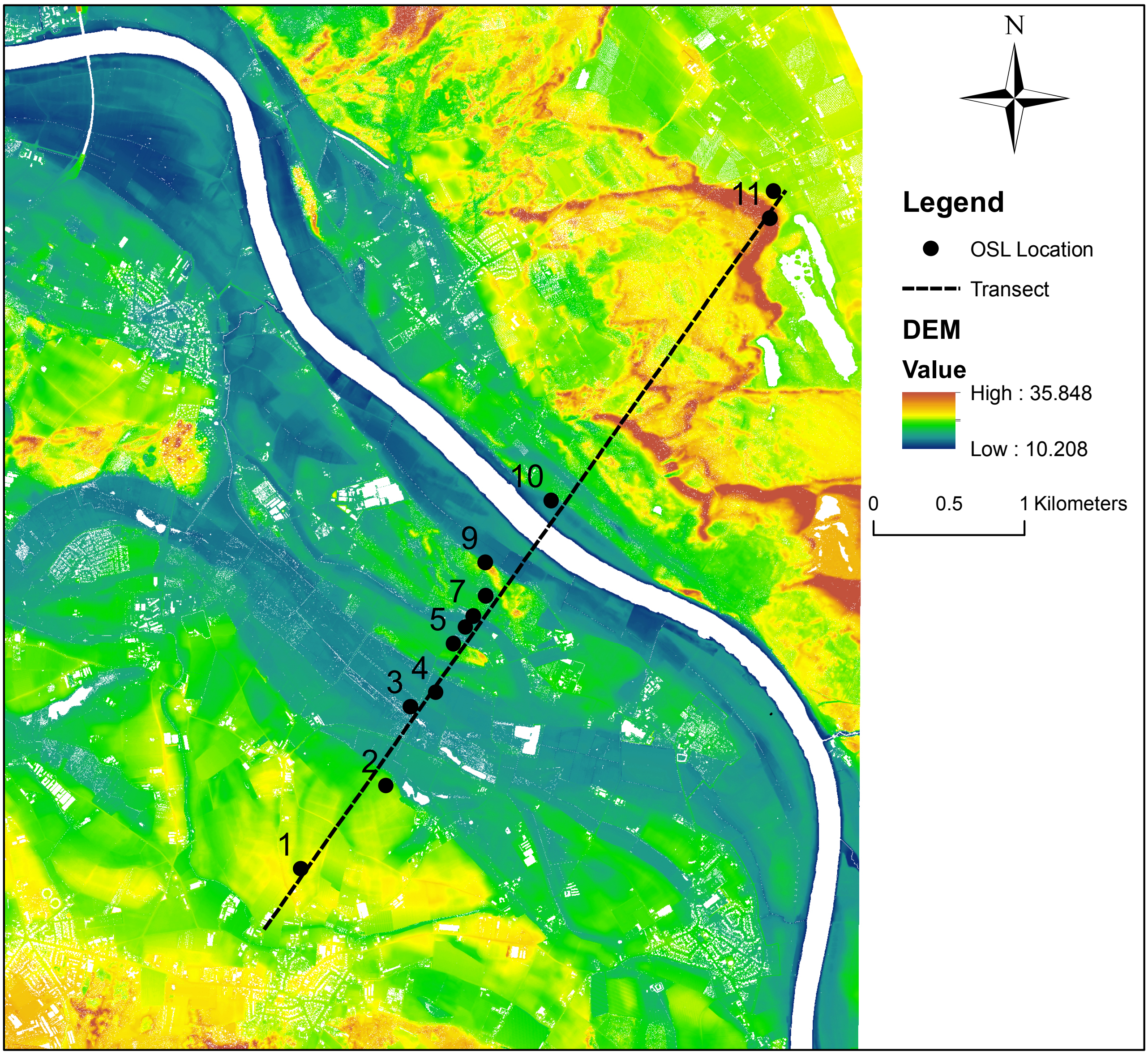

Figure 5.1: Digital elevation model of the study area and the transect with the OSL sampling locations. DEM adapted from the AHN (www.ahn.nl).

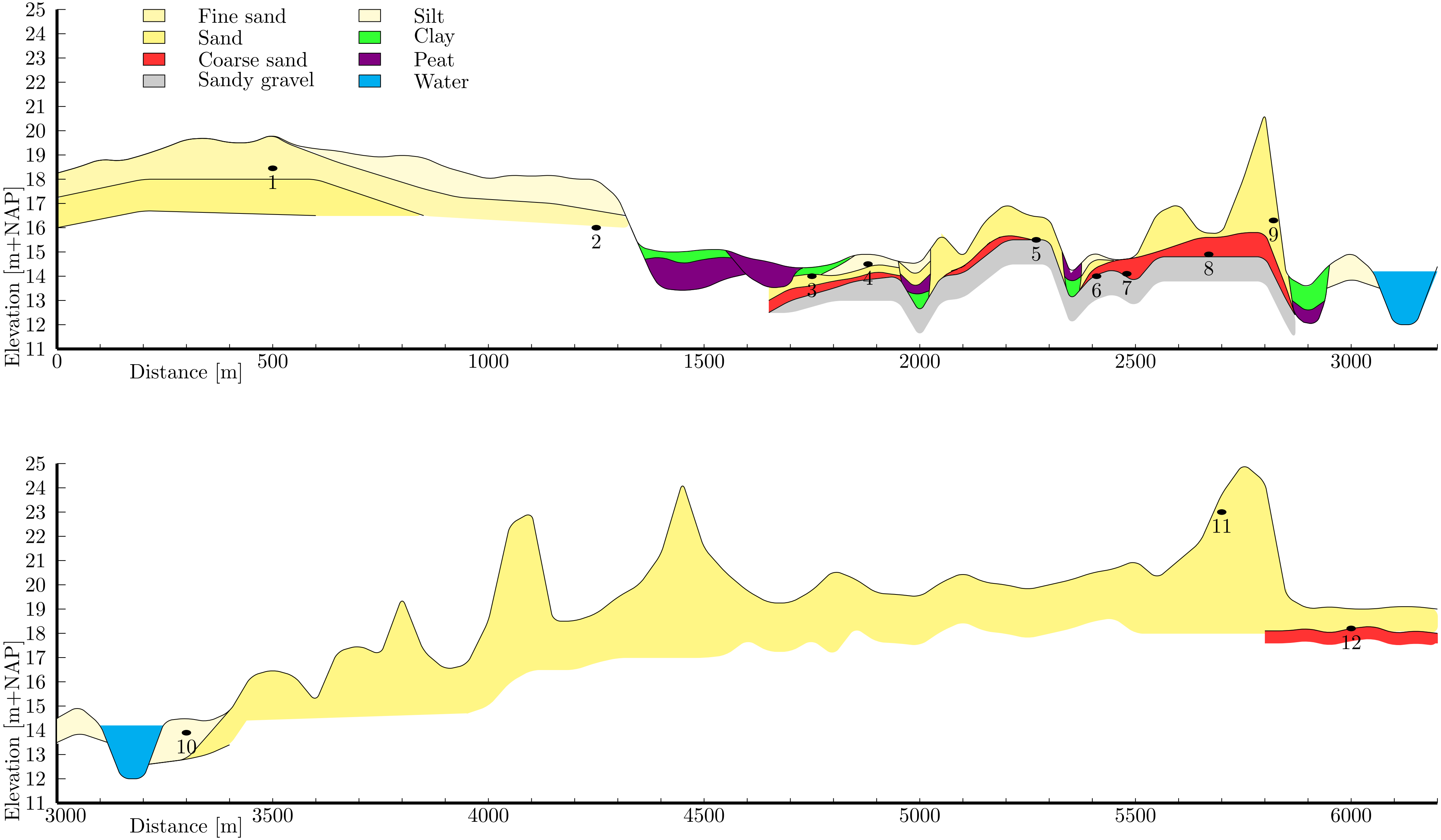

Figure 5.2: Lithological cross-section along the transect. The dots represent the OSL sampling locations with their corresponding depth.

Table 5.1: Genesis and elevation of sampling locations and depth below surface and expected age of the samples.

Location	Deposition	Surface Elevation (m)	Depth (m)	Expected age
1	Fluvial	19.66	1.30	Bølling
2	Fluvial	18.71	1.94	Bølling
3	Fluvial	14.21	0.36	Younger Dryas
4	Fluvial	14.77	0.56	Younger Dryas
5	Fluvial	16.19	1.20	Allerød
6	Fluvial	15.35	1.00	Younger Dryas
7	Fluvial	14.43	0.58	Younger Dryas
8	Fluvial	16.18	1.20	Allerød
9	Aeolian	19.03	1.45	Younger Dryas
10	Fluvial	14.33	0.78	Late Holocene
11	Fluvial	18.92	0.74	Bølling or Pleniglacial
12	Aeolian	28.72	0.76	Younger Dryas

5.2 Sample collection

When collecting sediments for OSL measurements, it is crucial to make sure that the sediment is not exposed to any daylight. Two sampling methods were used to ensure this during collection of the samples. The first method, the conventional one, consists of digging a trench until the layer of interest is exposed. After that an opaque plastic tube is inserted horizontally in this sediment layer. This tube is excavated and both ends are sealed to ensure that the sand in the middle of the tube is not exposed to any light. The second method is to collect the sediment from an auger hole. The main advantage of this method is that no trench has to be dug. This is done with an adjusted Edelman auger. The first step is to drill a hole until the layer of interest is reached. Secondly, an extension with a plastic tube is attached to the auger. This tube is pushed vertically down into the auger hole and into the sediment of interest. A disadvantage of this method is that it is less clear what layer is sampled, but some insight may be attained by drilling some deeper observation auger holes close to the hole where the sample will be collected. Another disadvantage is that these samples are taken vertically, resulting in a larger possible age range for the sediments.

The trench method was preferred because this provides a clear view of the sediment that is sampled. Both methods were used. Trenches were dug when possible, otherwise the auger method was used on locations where digging of a trench was not possible due to land use or ownership.

When determining at what depth the sample should be taken, it is important to ensure that the sediment has not been influenced by (bio)turbation. It is preferred to sample from a layer that still shows the layering that is characteristic for fluvial deposits. Doing so ensures that no material from different layers/ages has been mixed. Organic matter is also an indication of biological activity and therefore sediments containing organic matter are less suitable for OSL. A second property that has to be considered is the homogeneity of the layer that is going to be sampled. This is to ensure an uniform radiation field and a clear definition of the dose rate. Preferably the sample should be taken from a homogeneous layer with a thickness of at least 50 cm (Preusser et al., 2008).

When collecting the samples in the field, notes were made concerning the depth from where the sample was taken, the thickness of the layer where the sample was taken from and a lithological description of the layer. Besides these remarks also the coordinates, landscape position and possible remarks concerning the location were noted down.

5.3 OSL analysis

The OSL analysis to derive the age of burial of the sediments was done at the NCL (Netherlands Centre for Luminesence dating) located at the Wageningen University. The first step in the lab was removing the sediment from the sampling tubes. The outer ends of the sediment in the tubes were exposed to light during sampling. At least three centimeter of sediment was removed from each end of the tube, this sediment was set aside to be used for the dose rate measurements. The end result of this first step was a set of two subsamples of each sample: one subsample with (partially) light-exposed sand, used for determining the dose rate and one subsample consisting of sand that has remained in the dark, used for determining the palaeo dose.

5.3.1 Dose rate

For dose rate determination mainly sediment from the outer ends of the tubes was used. First, the sediment was dried at 105 °C for eight hours to remove all the water and hence to determine the water content of the sediment by weighting the sample before and after the heating. Next step was to remove the organic fraction in the sediment. This was done by ashing. The sediments were heated to 500 °C and kept at that temperature for eight hours. The organic matter content was determined by weighting the sample before and after the ashing. After the removal of both moisture and organics, the sediment was ground and sieved, so only the <300 μm fraction remained. This sieved sediment was mixed with liquid wax and crafted into a 9-cm-diameter puck with a thickness of 2 cm. The pucks were placed for 24 hours in a gamma spectrometer to measure the activity concentrations of radio nuclides and hence determine the dose rate. The dose rate was corrected for the moisture and organic content of the sediment.

5.3.2 Palaeo dose

The first step in the process of determining the palaeo dose was sieving of sediment. Grainsize 212-250 μm was used for the palaeo dose measurements, because this coarser fraction may have less problems with partial bleaching due to easier counting of the number of grains on a disc (Rittenour, 2008; Wallinga, 2002). To purify the quartz, several chemical treatments were done. HCl was added to remove carbonates, H_2O_2 to remove organic material and HF was applied to dissolve feldspars and to remove the α-irradiated part of the grains. To check the purity of the sample, an IR-test has been done to check for feldspar contamination (Duller, 2003).

Fluvial sediment may have problems with partial bleaching (Wallinga, 2002). To deal with partial bleaching, small-aliquots ($<$ 100 grains) were used as a proxy for single grain aliquots (Rittenour, 2008). The measurements were made using a RisøTL/OSL DA-20 reader (Bøtter-Jensen et al., 2003). The Single-Aliquot Regenerative (SAR) dose procedure (Murray and Wintle, 2000) was used for dose determinations. A preheat plateau test was done one three aliquots of each sample in order to select the proper preheat and cutheat temperatures. All samples were given a preheat of 240 °C and cutheat of 220 °C, except sample 10, which had 200 °C and 180 °C respectively. Rejection criteria for each measurement were recycling ratio 10 %, test dose error 10 % and palaeo dose error of 10 %. The goal was to maintain at least ∼25 aliquots of each sample that passed those criteria.

5.3.3 Age model

The next step in calculating the age of a sample was to derive one palaeo dose estimate from the distribution of the $>$ 25 aliquots measured. This is done with age models (Galbraith et al., 1999). Two age models were considered in this research: the central age model (CAM) and the bootstrapped three component minimum age model (MAM3, but referred to as MAM) (Galbraith et al., 1999; Cunningham and Wallinga, 2012). The MAM is useful in fluvial environments because it focuses on the well-bleached part of the population (Cunningham and Wallinga, 2012). The MAM requires three input parameters: the σ_b (%), σ_b error (%) and a start value (Gy).

The application of these age models used in this study can be divided in two phases (figure 5.3). In phase 1 the CAM is run for each sample. The result are two sets of 12 values: the palaeo dose estimate (CAM_x) and the overdispersion of each sample (OD_x). The overdispersion of a sample accounts for the amount of scatter in the dose from sources other than partial bleaching and counting statistics (Cunningham et al., 2011). After the CAM runs the resulting overdispersions are used as input for a MAM run (start = 0 Gy and $\sigma_b = 0 \pm 0$). The result of this run is one overdispersion estimate. In phase 2 the MAM is run for each sample. The MAM seems to be sensitive to low start values, causing the MAM dose estimate to become too low. Hence, the start value used is the corresponding CAM palaeo dose calculated in phase 1 (CAM_x). The σ_b used is the value obtained at the end of phase 1. The end result of phase 2 is a palaeo dose estimation (MAM_x) for each sample. The MAM was run multiple times for each sample to check if the palaeo dose estimate was stable.

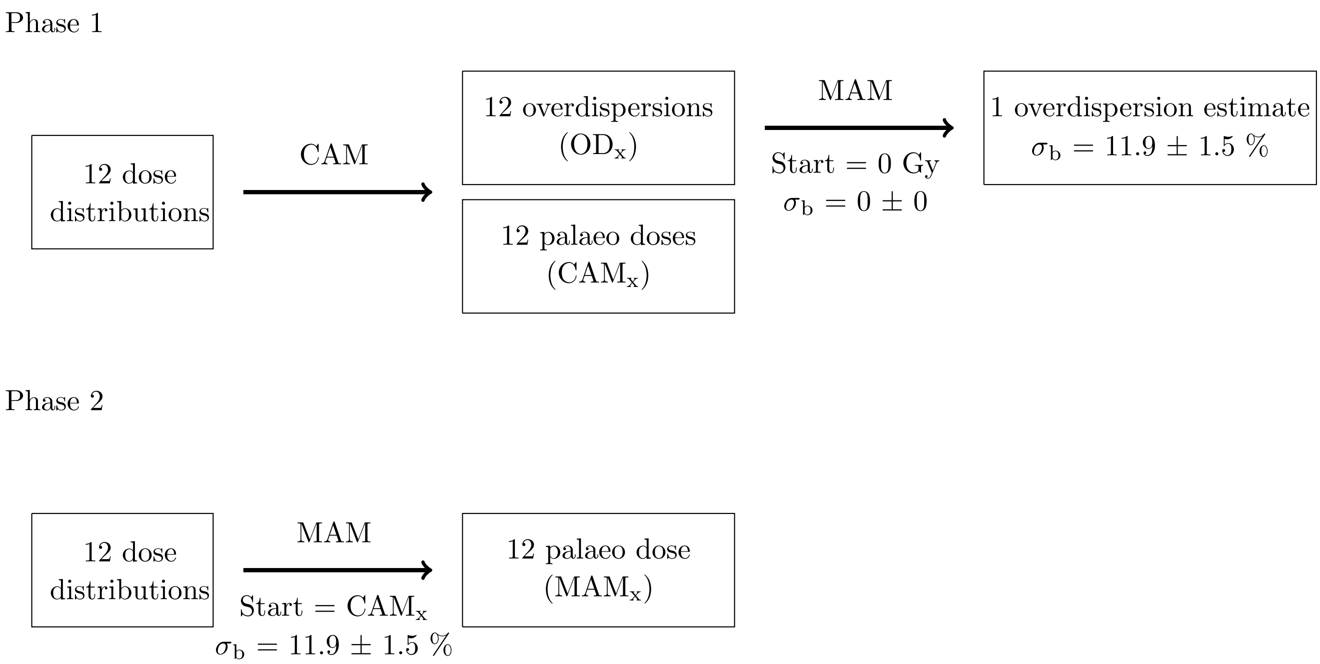

Figure 5.3: Schematic presentation of the application of the age models in this study.

5.3.4 Age determination

When the right palaeo dose has been determined with the age model and the dose rate is known, the age can be calculated with a simple calculation (equation 5.1). The resulting age is expressed in calender years before present.

$$Age\ (yr) = \frac{Palaeo\ dose\ (Gy)}{Dose\ rate\ (Gy/yr)} \tag{5.1}$$

Chapter 6

Results

In this chapter the results of the optically simulated luminescence measurements are presented. First, the results of the dose rate measurements will be given. Secondly, the results of the preliminary tests (IR and preheat-plateau) will be shown. These results were important in the following procedure to determine the palaeo doses of the samples. The result of the palaeo dose measurements will be presented after the results of the tests. From the dose distribution one dose should be extracted, this is done with age models. These resulting doses and the final ages of the sediments will be presented last.

6.1 Dose rates

The results of the dose rate measurements are shown in table 6.1. The water and the organic matter (OM) content and their errors have been estimated based on the values obtained by drying and ashing of the sediments (chapter 5.3). The depth was required to estimate the cosmic component of the dose rate. The final dose rate was calculated by taking into account the attenuation of the water content and organic matter. There is quite some spread in the dose rates observed in this study, ranging from 0.64 to 1.94 Gy/ka. The higher dose rate seem to be connected to the finer sediments.

Table 6.1: Results of the measurements and the data used in the calculations for the dose rates of the samples.

Sample	Dose rate (Gy/ka)	Depth (m)	Sediment	Water content (%)	OM (%)
1	1.96 ± 0.07	1.30	Fine sand	7 ± 3	1 ± 0.25
2	0.89 ± 0.06	1.94	Fine sand	5 ± 2	1 ± 0.25
3	1.68 ± 0.06	0.36	Clay	25 ± 5	2 ± 0.5
4	0.86 ± 0.03	0.56	Fine sand	15 ± 5	0 ± 0
5	1.13 ± 0.04	1.20	Fine sand	7 ± 3	1 ± 0.25
6	0.77 ± 0.03	1.00	Coarse sand/gravels	25 ± 5	1 ± 0.25
7	0.73 ± 0.03	0.58	Coarse sand/gravel/peat	25 ± 5	3 ± 0.75
8	0.83 ± 0.03	1.20	Coarse sand	5 ± 2	0 ± 0
9	0.64 ± 0.02	1.45	Coarse sand	5 ± 2	0 ± 0
10	1.31 ± 0.04	0.78	Silt	12 ± 3	1 ± 0.25
11	0.66 ± 0.02	0.76	Sand	5 ± 2	1 ± 0.25
12	0.67 ± 0.02	0.74	Sand	15 ± 4	1 ± 0.25

6.2 Palaeo dose

The first step in determining the palaeo doses was to check whether the measurement procedure was working correctly. The results of the IR-test and the dose recovery test will be presented. These results of these test are important indicators of the reliability of the OSL signal in the Meuse sediment. After these tests, the actual dose measurement results, the dose distributions, will be given. Next step was to derive one dose from this distribution with the use of age models.

6.2.1 IR-test

The extracted quartz fraction showed no response to IR stimulation. This means that contamination by feldspar luminescence can be excluded.

6.2.2 Dose recovery test

The results of the dose recovery test are shown in table 6.2. The test was performed with a preheat of 240 °C. The aliquots were given a dose of 8.85 Gy from a laboratory beta source. The mean recovery ratio of each sample was calculated from a set of three aliquots. The results are all centered around unity. The mean recovery ratio for all the samples, based on 32 accepted aliquots, is 0.99 ± 0.05. The error of sample 3 is higher than the other samples because it was measured on a smaller disc size (2 mm compared to 5 mm for the other samples).

Table 6.2: Results of the dose recovery test. For each sample three aliquots with a 5 mm mask were measured, the table shows mean values. Sample 10 was not measured due to the expected young age.

Sample	Dose recovery ratio
1	1.01 ± 0.02
2	0.96 ± 0.02
3 [a]	1.04 ± 0.23
4	1.01 ± 0.02
5	0.97 ± 0.01
6	0.98 ± 0.04
7	1.02 ± 0.09
8	0.98 ± 0.01
9	0.99 ± 0.04
10	
11	0.97 ± 0.06
12	0.96 ± 0.06

[a] Measured on aliquots with a mask of 2 mm

6.2.3 Dose distributions

For each sample at least 25 aliquots had to pass the rejection criteria (see chapter 5.3). In figures 6.1 and 6.2 kernel density plots (KDE plot) of the dose distributions are shown. The most important aspect of the plots are the black dots (individual aliquots dose) and their error bars (one standard error). The results of the age models are also indicated by the red dashed (CAM) and blue lines (MAM), see section 6.2.4. Samples 2, 3 and 9 have more measured aliquots than the other samples. The amount of aliquots measured for the other samples was less due to time constrains, but still pass the criteria of > 25 accepted aliquots. For the radial plots of the samples the reader is referred to appendix B.

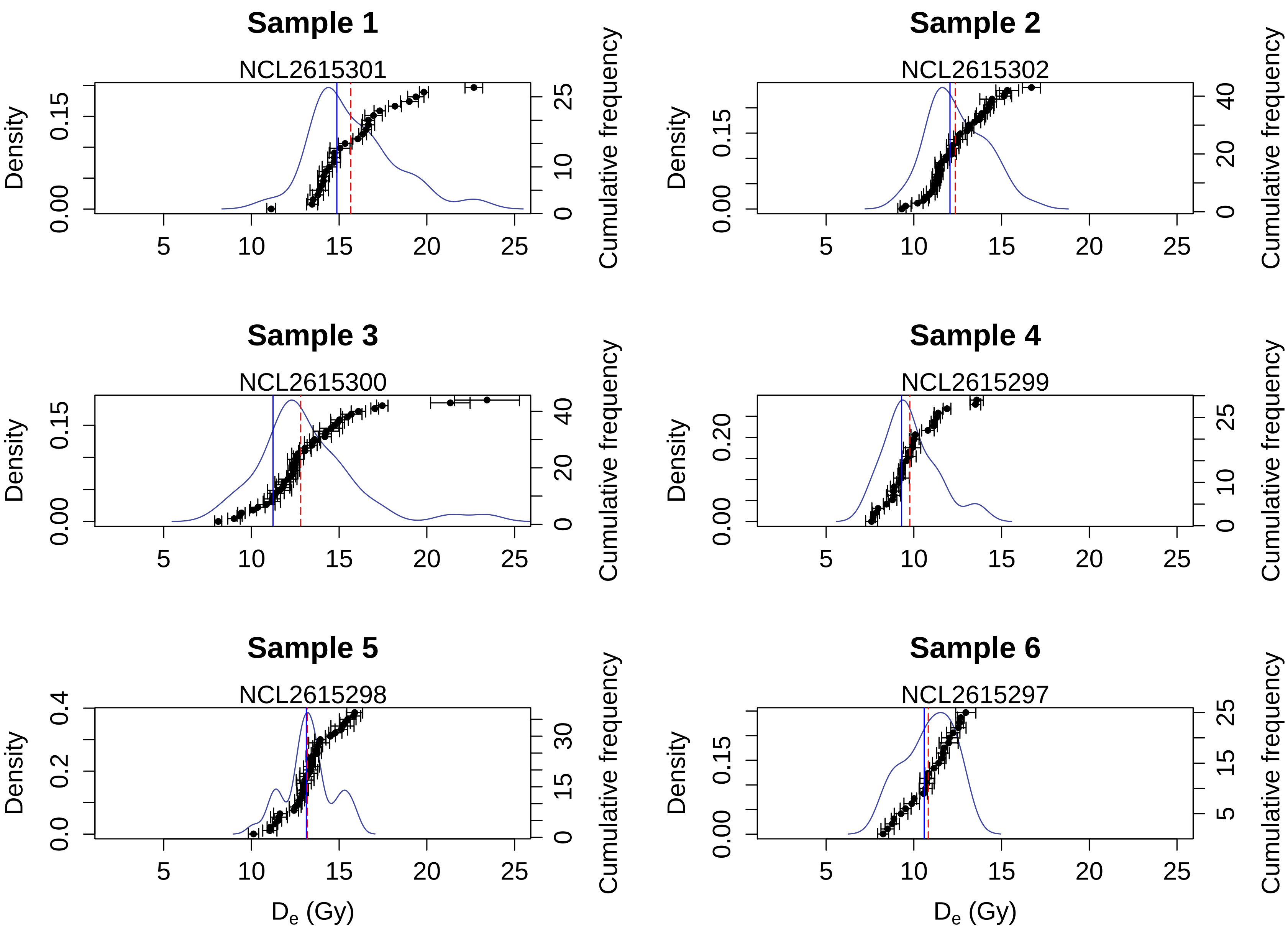

Figure 6.1: KDE plots of samples 1-6. The blue line indicates the MAM dose and the red dashed line indicates the CAM dose.

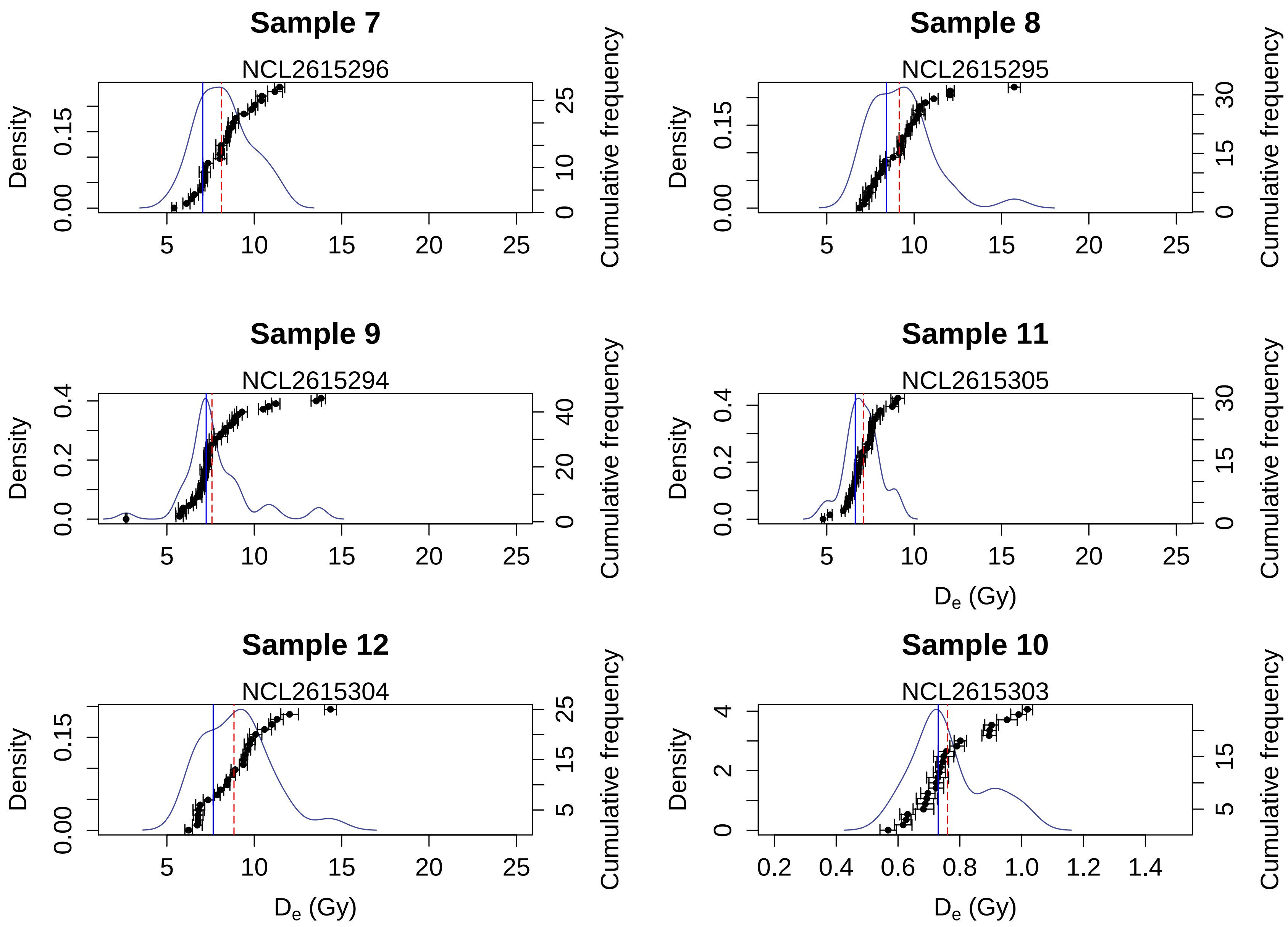

Figure 6.2: KDE plots of samples 7-12. The blue line indicates the MAM dose and the red dashed line indicates the CAM dose. Mind the different x-axis of sample 10.

6.2.4 Age calculations

Two age models were used in this research, the central age model (CAM) and the minimum age model (MAM). For their exact application the reader is referred to the methods section (chapter 5.3.3). In table 6.3 the outcomes of both age models, the dose rates and the resulting ages are shown. In figure 6.7 the ages are placed on the cross-section for a clear overview. The final ages of the samples are based on the outcome of the minimum age model. This ensures that the age is not influenced by poorly bleached grains. When a sample is well bleached, the CAM will be approximately the same as the MAM. The CAM/MAM ratio (table 6.3) gives an indication for the bleaching of the sample.

A disadvantage of the MAM is that it is influenced by low (young) outliers. These young outliers can be caused by mixing of the sample with younger material. These have to be removed from the samples population in order to get a good estimate from the MAM. In figures 6.1 and 6.2 the outliers are still visible, but they are not used as input for the ages models. The following samples have had some outliers removed: samples 1, 9 and 11. The removal of these outliers resulted in a higher MAM dose, which resembled the population better.

For the aeolian samples (9 and 11) there has been some further analysis of the application of the MAM. Due to the generally better sorting, the effect of micro dosimetry is smaller in aeolian sediments, resulting in a lower overdispersion (OD) when compared to fluvial sediments. The overdispersion calculated with the CAM does suggest the opposite for the samples under consideration in this research (table 6.3). However, the effect of a lower overdispersion is still evaluated for the aeolian samples. The overdispersion of the CAM was used as an input parameter in the MAM in the form of σ_{b}. The σ_{b} used for all the samples was 0.12 (12%). However, for the aeolian samples an experiment with lowering the σ_{b} (based on the theoretically lower OD of aeolian samples) have been performed to see whether this would improve the age estimation by the MAM. The σ_{b} has lowered by 5 %, from 12 % to 7 %. The effects of this variation in MAM input are the clearest when looking at the radial plots of the aeolian samples (figures 6.3 - 6.6). The lowering of σ_{b} results in a lower dose. For both samples this does seem to give a underestimation of the palaeo dose. This can be seen in figures 6.4 and 6.6. The gray bar (palaeo dose) misses the lowest points, indicating a underestimation of the palaeo dose. Hence, all the MAM ages are calculated with a σ_{b} of 12%.

Table 6.3: Results of the age model runs and the resulting age, based on the MAM. The uncertainties are given in two standard errors.

Sample	Lab code	CAM (Gy)	OD (%)	MAM (Gy)	CAM/MAM	**Age (ka ago)**
1	NCL2615301	15.7 ± 0.9	14.04	14.9 ± 1.4	1.05	**7.58 ± 1.54**
2	NCL2615302	12.4 ± 0.5	11.57	12.1 ± 0.8	1.02	**13.5 ± 2.66**
3	NCL2615300	12.8 ± 0.7	17.97	11.2 ± 1.7	1.14	**6.66 ± 2.12**
4	NCL2615299	9.71 ± 0.62	13.8	9.30 ± 0.76	1.04	**10.8 ±2.02**
5	NCL2615298	13.5 ± 0.80	8.94	13.1 ± 0.5	1.03	**11.6 ± 1.26**
6	NCL2615297	10.8 ± 0.5	10.97	10.6 ± 0.9	1.02	**13.8 ± 2.62**
7	NCL2615296	8.13 ± 0.56	17.46	7.05 ±0.84	1.15	**9.66 ± 2.44**
8	NCL2615295	9.33 ± 0.78	17.31	8.41 ± 0.90	1.11	**10.07 ± 2.30**
9	NCL2615294	7.58 ± 0.58	24.7	7.25 ±0.36	1.05	**11.3 ± 1.42**
10	NCL2615303	0.76 ± 0.02	13.73	0.73 ± 0.06	1.04	**0.56 ± 0.1**
11	NCL2615305	6.95 ± 0.36	13.03	6.63 ± 0.76	1.05	**10.0 ± 2.40**
12	NCL2615304	8.84 ± 0.70	19.17	7.65 ± 0.55	1.16	**11.5 ± 1.90**

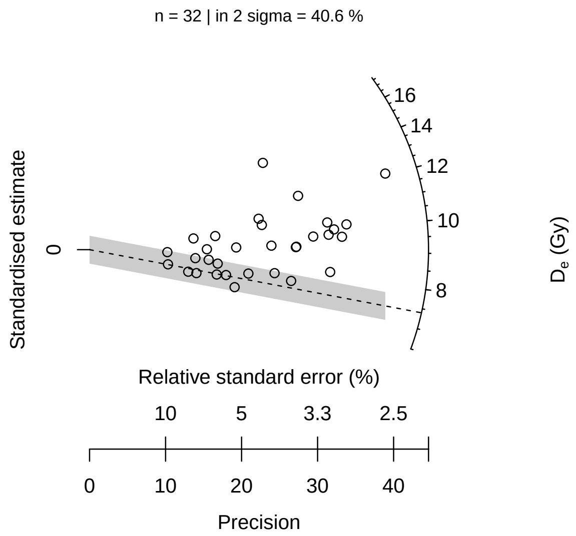

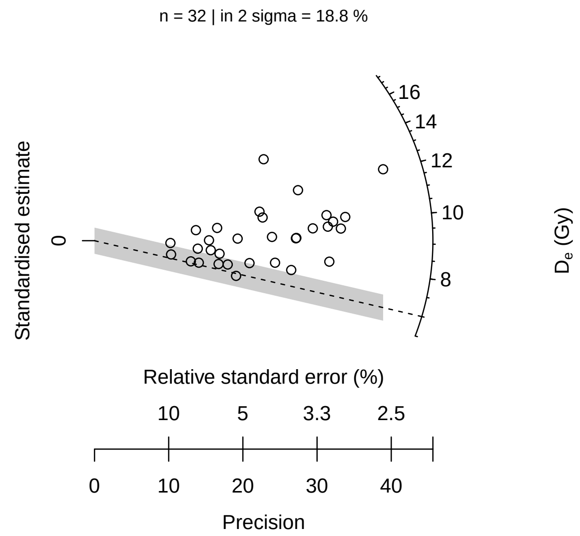

Figure 6.3: Radial plot of sample 9 (NCL2615294) with $\sigma_{\mathrm{b}} = 12\%$

Figure 6.4: Radial plot of sample 9 (NCL2615294) with $\sigma_{\mathrm{b}} = 7\%$

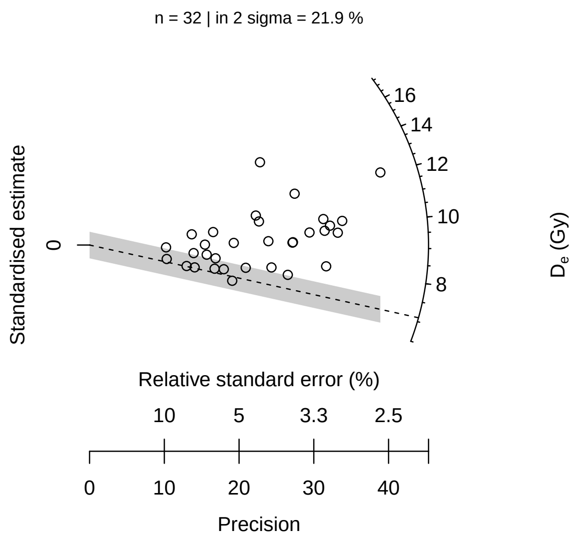

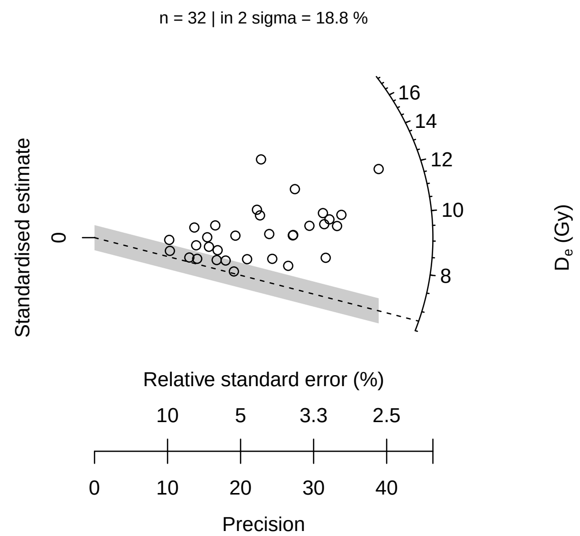

Figure 6.5: Radial plot of sample 11 (NCL2615305) with $\sigma_{\mathrm{b}} = 11\%$

Figure 6.6: Radial plot of sample 11 (NCL2615305) with $\sigma_{\mathrm{b}} = 7\%$.

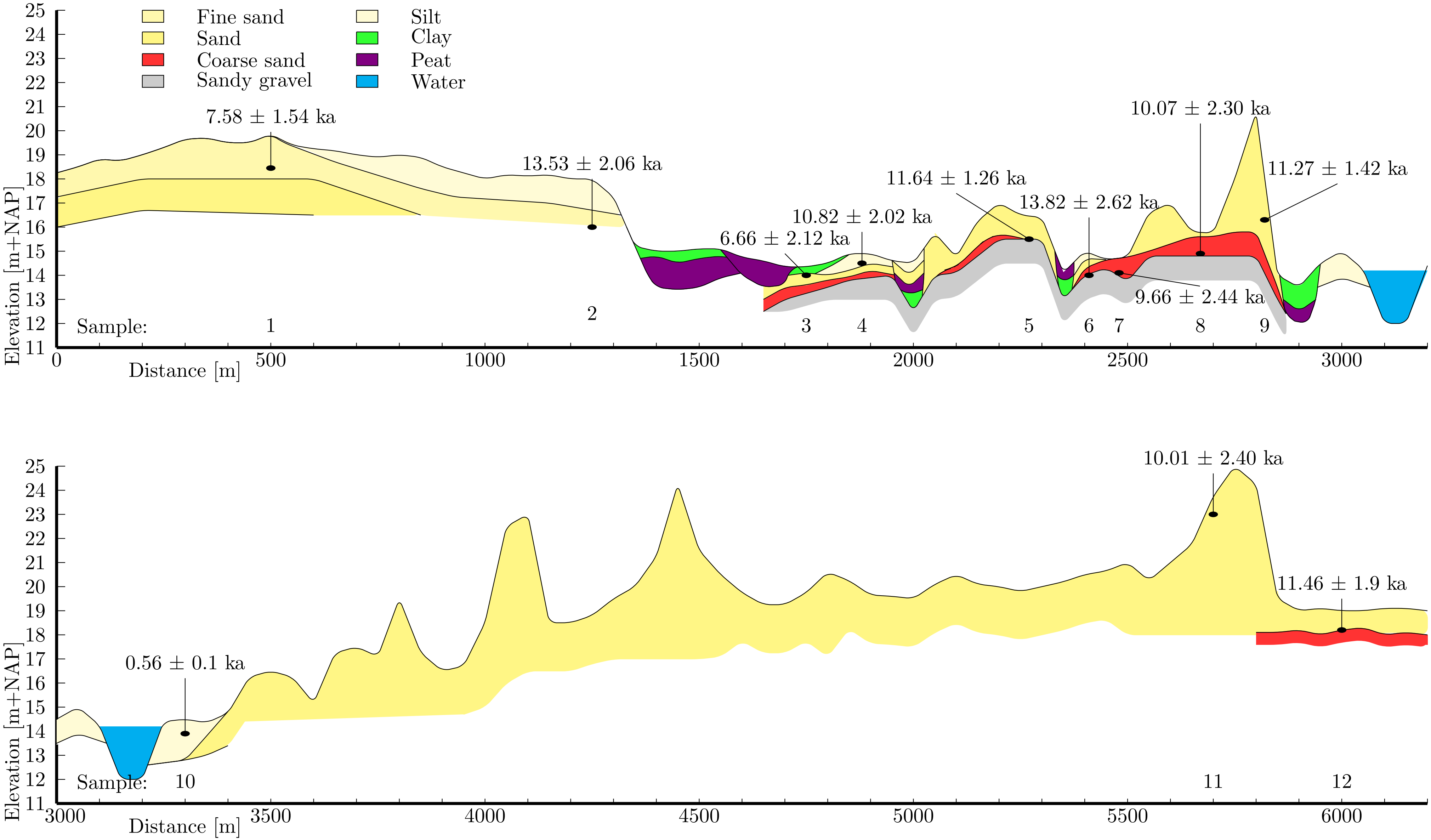

Figure 6.7: Lithological cross-section with the locations of the samples and their corresponding ages.

Chapter 7

Discussion

In this chapter the results form chapters 4 and 6 will be discussed. First, the auger data and the constructed cross-section will be discussed. This is followed by an analysis of the OSL results. Following the discussion of the OSL results, there are two possible fluvial response theories based on the OSL ages. These are compared to the work of Huisink (1997) and Tebbens et al. (1999).

7.1 Cross-section

7.1.1 Problems

The cross-section was based on 40 augering spread over a length of 6 km. The maximum depth of the augering was 2.5 m but often this was not reached due to some problems encountered during the augering. These problems include the presence of gravels, obstructing the auger. Some location were too wet, the sediment were not solid enough to stay in the auger/guts. The same applies for sediments that were too dry, especially the fine sand. The depth of the augering seems sufficient for the larger part of the western section of the cross-section. Although it would have been better to be able to go a bit deeper on the highest terrace level to find the gravels. To get a better understanding of the fluvial terraces that might be present on the east bank of the Meuse, deeper augerings are required. This might be quite difficult due to the thick layer of aeolian sand. This sand is difficult to auger due to the instability of the auger hole.

7.1.2 Morphological units

There are several geomorphological units that can be distinguished when looking at the cross-section (figure 6.7). There is the highest terrace level spanning from 0 to 1300 m and continuing at 5900+ m. These two parts are separated by an incision of the Meuse (1300 - ~4000 m). This incision can be divided in several subparts. From 1300 to 2000 m is the lowest and wettest part of the terrace sequence. The peat and clay indicate that channels have been abandoned and have been filled with peat and clay. There is a small river terrace as well (1800-1900 m). East of this lowest part are several terrace remnants (2000-2900 m) with aeolian deposits on top of them. These remnants are incised by several channels. These channels are now filled with clay and peat. Next to these terrace remnants is the current floodplain of the Meuse (2900 - 3300 m). East of the Meuse are some small terrace remnants (3400 m), but most of these are covered by the parabolic river dunes (3300 - 5900 m).

7.2 OSL procedure

The results of the IR-test confirm that there are no remaining feldspars in the chemically threated samples. The preheat temperatures that were selected for the samples were based on a small preheat test. Only three aliquots of each sample were tested for each temperature. Due to the selection criteria some of these aliquots were rejected, resulting in even less data and some gaps in the data. However, there are no reasons to assume that age errors arise due to the used preheat. The results of the palaeo dose measurements did not show signs of thermal transfer with the preheat temperatures used.

7.2.1 Bleaching

Some samples did show some signs of incomplete bleaching. When looking at the KDE plots (figures 6.1 and 6.2) there are some older outliers. Some clear examples are sample 3 and 8. The central age model is sensitive for the high outliers. They cause an older age for the sample. The result is a difference between the CAM and the MAM, expressed in the CAM/MAM ratio (table 6.3). In well-bleached samples this ratio should be around unity. This is the case for most of the samples. For the samples that did have some non-bleached aliquots, the MAM seems to give a good estimate of the true dose. Partial bleaching did not end up to be a serious problem as was expected at the start of the research.

7.2.2 Age Model

Due to some poorly bleached aliquots the MAM is preferred over the CAM. However, to get reliable values from the MAM low outliers had to be removed (e.g. in sample 9). When this was done the MAM results resembled the CAM for the well bleached samples. For the samples with poorly bleached aliquots the MAM gives a younger, more representable age that the CAM. Based on these observations, it was decided that the MAM will be used for all the samples to calculate the right dose. A disadvantage of the MAM is that the uncertainties of the age estimations are higher that those of the CAM (table 6.3).

7.2.3 Application of the MAM on aeolian samples

The division of the samples in aeolian and fluvial samples when applying the age model was based on the concept of the grade of sorting of the sediments and hence the overdispersion. According to Murray and Roberts (1997) there are several factors that can influence the dispersion: anomalous fading, thermal transfer, reworking of sediment, variations in luminescence response to laboratory treatment and variations in microdosimetry. In this research several of these factors can be excluded. Anomalous fading will have had no influence, because only quartz was measured in this research (Rittenour, 2008). Thermal transfer due to the preheat is also discarded as a source of scatter based on the criteria mentioned by Murray and Roberts (1997). The reworking or mixing of sediment can be a factor that plays a role in the overdispersion in this research. However, the samples were taken at such a depth to avoid (recent) bioturbation and reworking by human activity (ploughing etc.). The results of the preheat plateau test dismiss the possibility of each grain responding differently to the given preheat. The last factor of influence is the variation in microdosimetry. This is a result in grain-to-grain variation in the dose rate (Olley et al., 1997). When a sediment is well sorted, the effect of microdosimetry decreases, generally resulting in a lower overdispersion. In theory aeolian samples are better sorted than fluvial samples, resulting in a more homogeneous radiation field and hence a lower effect of microdosimetry for aeolian samples. This leads to the hypothesis that aeolian samples should have a lower overdispersion than the fluvial samples. This would have an effect on the age calculated with the MAM (section 5.3.3).

The average overdispersion is 15.2% (table 6.3). For the aeolian samples it is to be expected that they have a lower overdispersion than the fluvial samples due to a more uniform radiation field. The 10 fluvial samples have a mean overdispersion of 14.5%. The two aeolian samples (9 and 11) have an overdispersion of 24.7% and 13.0% respectively. The aeolian OD's are not lower than the fluvial overdispersions, as would be expected. Sample 9 even has the highest OD (24.7%) measured in this research. This is unexpected for aeolian samples. The overdispersion of sample 9 is extremely high, but this is mostly due to the young outlier at 2.7 Gy (figure 6.2). When this young aliquot is removed the overdispersion returns to a more sensible value of 19%. Still the aeolian OD's are not lower than the OD's of the fluvial samples. A possible explanation for this unexpected aeolian overdispersions could be the transport distance of the aeolian deposits. The source area of the sediments that now form the river dunes were the (dry) riverbeds of the Younger Dryas Meuse (Huisink, 1997). This means that the transport distance of the sediments was not more than several hundreds of meters. Due to this short transport distance, there was little opportunity to separate the small from larger grains resulting in a badly sorted aeolian deposit, as observed in the field. This resulted in overdispersion comparable to those of the fluvial samples.

In conclusion there is no difference between the aeolian and fluvial samples based on overdispersion. This means that the same input is used for the MAM for both kinds of samples. However, the effect of a lower OD has still been investigated for the aeolian samples. The lower σ_b did not result in a better age approximation statistically. Comparing the radial plots of both aeolian samples (figures 6.3 - 6.6) it becomes clear that the original σ_b gives a better dose estimation. The lower σ_b causes a underestimation of the dose according to the radial plots.

7.3 Age interpretation

Before the ages are discussed it is important to get some knowledge about the way the ages should be interpreted. With OSL ages it should be kept in mind that it is a minimum age of the terrace that is sampled. The age indicates the time that has passed since the sampled sediment got buried. For river terraces this time of burial does not have to correspond with the floodplain abandonment / terrace formation. When a terrace is formed, it can still receive sediment from the river during peak discharges (figure 7.1). In order to get the age of the terrace formation, the sample should be taken at the right depth, below the overbank deposits that are deposited on the terrace (brown in figure 7.1). In the field this was not always clear, especially when collecting the OSL sample with the auger. The consequence of this is that the OSL-dated ages of the terraces might not correspond to the age of the formation of the terrace. Sampling of the flood deposits gives an age estimation of the incision of the younger, lower terrace. This should be kept in mind while interpreting the OSL ages.

The ages are divided in groups based on the units that were identified on the cross-section (see section 7.1.2). The following units and their OSL ages will be discussed (from west to east): the highest terrace level, lowest level, terrace remnants, Meuse floodplain and the river dunes. After the units are discussed a theory concerning the fluvial response during the Late Glacial is given and it is compared to the work of Huisink (1997) and Tebbens et al. (1999).

7.3.1 Highest level

The highest river terrace in the study area can be found at the west of the transect and probably at the eastern end of the transect. It is intersected by a 'valley' formed by the Meuse. Based on elevation these two terraces (east and west) can be connected. However, when looking at the OSL ages obtained from both ends, it becomes more complicated. Three ages are available for this wide terrace (figure 6.7): sample 1, 2 and 12 with their ages of 7.58 ± 1.54, 13.5 ± 2.06 and 11.5 ± 1.90 ka ago respectively. When trying to place these points in a chronozone, it becomes clear that these ages do not fit in one single chronozone (figure 7.3).

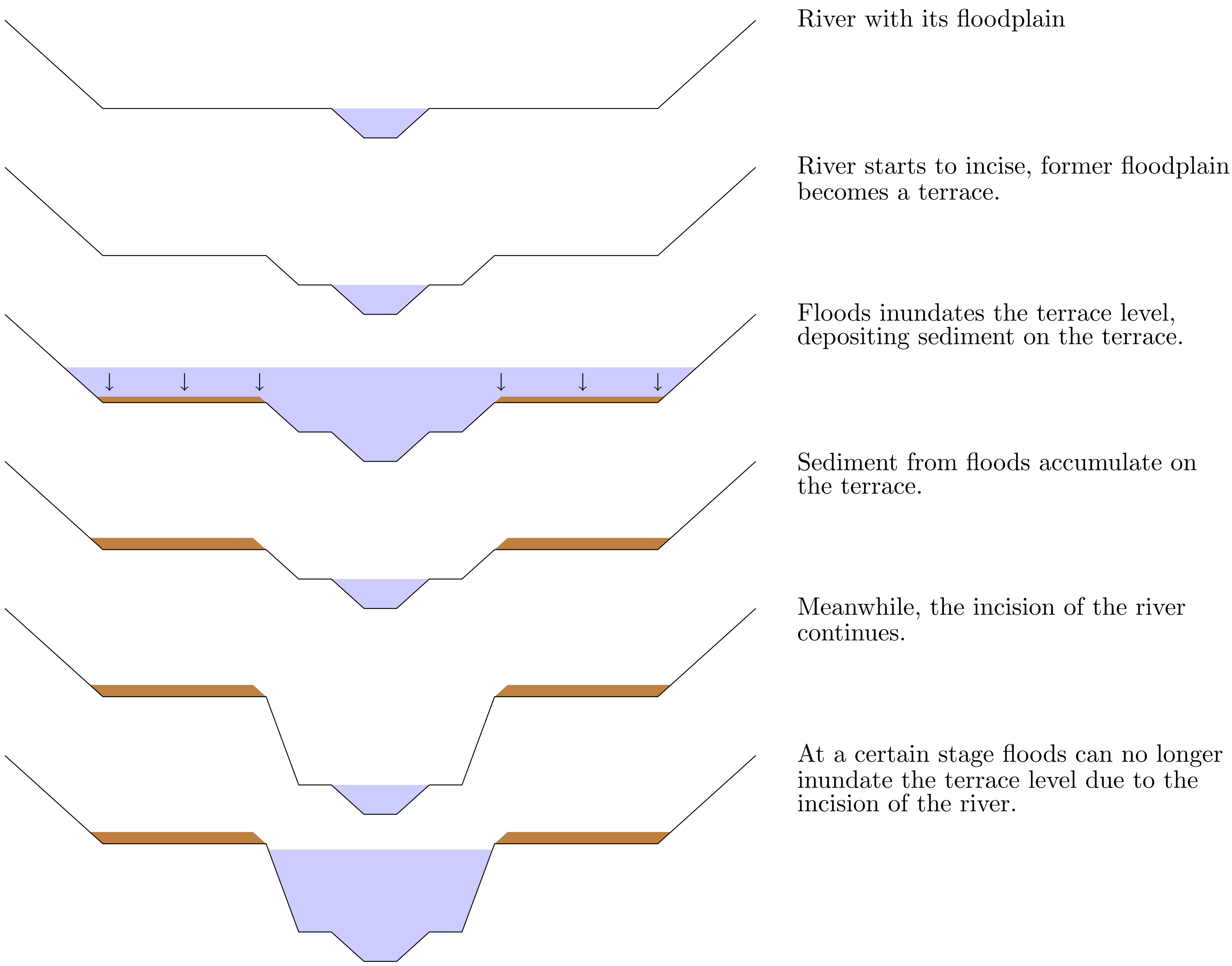

Figure 7.1: Schematic representation of an incising river that still influences the higher terrace level(s).

Starting with the youngest sample of this unit: sample 1. The Holocene age makes it rather unlikely that these sediments are deposited by the Meuse during the Holocene, due to the high position in the landscape. It is more likely that the sediments of the terrace have experienced some aeolian reworking during the Holocene. This explains the (unexpected) young age and might be the cause of the irregular relief (see figure 5.1) that can be found on this part on the terrace. Sample 2 offers a more likely age for the highest terrace level. This sample sets the minimum age of the terrace at the Late Glacial interstadial (Bølling-Allerød). Keeping in mind that this is a minimum age, it might lead to the conclusion that this is the Pleniglacial river terrace. However, the age of the sample 12 suggests that the terrace is younger, a minimum Younger Dryas/early Holocene age. When looking at the dose distribution of sample 12 (figure 6.2) it might be possible that the sample is somewhat older than the MAM suggest. This would give sample 12 an age comparable to that of sample 2, supporting the idea of a Pleniglacial terrace.

7.3.2 Lowest level

The lowest terrace level has two dates available: sample 3 and 4 with ages of 6.66 ± 2.12 and 10.8 ± 2.02 ka ago respectively. Sample 3 is the clay fill of a channel and has a mid-Holocene age while sample 4 seems to be a terrace level from the Younger Dryas or early Holocene. The Holocene sediments of sample 3 are mainly clays with some peat in it. These fine fills indicate a calm sedimentation environment. This might have been a Younger Dryas channel that filled during the Holocene when the Meuse flooded and fine overbank deposits were deposited in the abandoned Younger Dryas channel. Sample 4 is located on a location with a slightly higher elevation than the field of sample 3, indicating that it might be a different terrace. The age of sample 4 placed this higher terrace in the Younger Dryas/early Holocene. This probably means that it is a remnant from the Younger Dryas that experienced less incision and hence received less sediments during the Holocene due to its slightly higher elevation.

7.3.3 Terrace remnants

These terrace remnants are separated by an incision of a lower terrace remnant with a (filled) channel. Both the terraces (samples 5 and 8) and the fill of the channel (samples 6 and 7) have been dated, as well as the river dune that is present on the terrace of sample 8 (see section 7.3.5). Based on elevation both terrace remnants could be the same terrace intersected by the channel. However, at first sight the ages of both remnants are not corresponding (figure 7.3). Sample 5 is dated at the transition from the Younger Dryas to the Holocene (11.6 ± 1.26 ka ago) while sample 8 has an early Holocene age (10.1 ± 2.30 ka ago). There is hardly any overlap between the error bars, leading to the idea that these are two different terraces. However, the age of sample 8 might be too young. The river dune that lays on top of this terrace has an age of 11.3 ± 1.42 ka ago while the terrace is dated at 10.1 ± 2.30 ka ago. Stratigraphically the terrace should be older than the dune on top of it. This implies that the age of sample 8 should be older, making it more comparable to that of the other terrace remnant (sample 5). This makes the assumption of one terrace level a viable option again.

The dune on top of the terrace is most likely from the Younger Dryas (see section 7.3.5). This implies that the underlying terrace is at least of Allerød age. However, the ages of samples 5 and 8 suggest a Younger Dryas/early Holocene age for this terrace. Keeping in mind the principle of figure 7.1, these terrace remnants are probably from the Late Glacial interstadial, but could still be from the Younger Dryas.

The channel itself is dated as well, more precisely, the sedimentary fill of the channel is dated. Sample 7 is the channel fill and sample 6 is a lower terrace remnants between the other two interstadial remnants (figure 6.7). The channel has an age corresponding with the early Holocene (9.66 ± 2.44 ka ago). This minimum age of the channel suggests that the channel was active during the Younger Dryas and probably during high flows in the Holocene. The lower terrace level has an age of 13.8 ± 2.62

ka ago. Due to the high uncertainty it is hard to place this date in a certain chronozone (figure 7.3). The MAM places the age at the Bølling-Allerød transition, so this age is interpreted as a Late Glacial interstadial one. How is this age connected to the Late Glacial age that was found on the highest terrace level (sample 2)? Sample 6 might be a part of the interstadial Meuse floodplain that was not eroded away. Later, this erosion remnant was buried again by new (Younger Dryas) sediments. While the sediments of sample 2 probably are the overbank deposits of the floods of the interstadial Meuse, sample 6 might be the old interstadial floodplain (figure 7.1).

7.3.4 Meuse floodplain

The current floodplain of the Meuse is quite narrow in the study area. One sample was taken from the eastern levee (Sample 10). This resulted in an age of 0.56 ± 0.10 ka ago taken at a depth of 0.8 meter. It provides an indication of the average sedimentation rate over at least the last 500 years.

7.3.5 River dunes

There are two river dunes sampled in this research. One smaller dune (sample 9) and one of the large parabolic dunes found on the east bank of the Meuse (sample 11) were dated. The smaller dune is dated at 11.3 ± 1.42 ka ago. This means that the dune was active until the early Holocene. The highest activity was probably during the Younger Dryas due to the more favorable aeolian conditions during that time. At the start of the Holocene vegetation started to recover (Bohncke, 1993) and the dune became stable.

The eastern parabolic aeolian structures have also been dated. Sample 11 had an age of 10.0 ± 2.40 ka ago. Just as the other dune (sample 9), the Younger Dryas is the most logical period for the formation of these dunes. However, due to the larger scale of this system compared to the small dune of sample 9, it might be possible that it remained active for a longer time due to the self-enhancing effect of this large system. This means that vegetation grow lagged, keeping the dune active until the early Holocene. This explains the younger age of the larger dune.

The fact that the OSL dating places both dunes in the Younger Dryas can be used as a reference point. The OSL ages correspond with the expected ages of the dune complexes. This gives confidence in the reliability of the OSL ages.

7.4 Late Glacial River response

7.4.1 Pleniglacial

The large terrace is dated to the Pleniglacial (section 7.3.1). Such a wide floodplain suits the braided river style that was characteristic for that time. The sparse vegetation and generally dry conditions favored high sediment supply and sporadic discharge, promoting an aggrading braided river system (figure 7.2).

7.4.2 Bølling-Allerød (Late Glacial interstadial)

The Bølling and Allerød interstadials are separated by the colder Older Dryas. As mentioned earlier, this period is often not represented in geological archives. In this research no sediments or terraces from this period were found and the resolution of the OSL dating method is too small to identify this chronozone. There is no difference between Bølling and Allerød terraces based on ages due to the uncertainty in the OSL results. Therefore the Bølling and Allerød are taken together as one interstadial in this study.

The warming at the transition from the Pleniglacial to the Bølling interstadial and an increase in precipitation caused vegetation to grow and created a more regular discharge regime for the Meuse. The decrease in sediment load and a more regular discharge caused the Meuse to adapt its morphology to a more meandering single-channel system. The Meuse started to incise in the thick sediment of the braided Pleniglacial floodplain (figure 7.2). This is the 'valley' that can be found in the highest terrace level. This was the first major incision phase of the Late Glacial, at a cold-to-warm transition.

The terrace remnants that are found in the valley (section 7.3.3) are probably from the interstadial. It is hard to estimate how deep the incision was of this interstadial Meuse caused by the cold-to-warm climatic transition. This is due to the problem with identifying the exact terrace height due to later sedimentation on a terrace level (figure 7.1).

7.4.3 Younger Dryas and Holocene

Based on the cross-section (figure 6.7), two major incision phases are expected. The first phase formed the large valley incision in the highest terrace level during the Bølling/Allerød interstadial, as discussed above. The second incision phase was responsible for the incision into the terrace level of the terrace remnants. The exact timing of this second incision phase is unclear. From figure 7.3 it becomes evident that the Younger Dryas and especially the early Holocene was a period of high fluvial and aeolian activity. For the fluvial activity, there are three options for the timing of the second incision phase: (1) at the warm-to-cold transition from the Allerød to the Younger Dryas, (2) at the cold-to-warm transition of the Younger Dryas to Holocene and the last option (3) is that at both mentioned climatic transitions an incision phase took place. Each fluvial scenario will be discussed here, as well as the river dunes that were formed during this period.

Scenario 1

The first scenario (Allerød-Younger Dryas) assumes an incision phase as a reaction to a changing discharge regime with a lagging vegetation change at the start of the Younger Dryas. This incision should have taken place in the interstadial terrace/floodplain (figure 7.2). This would have been the terrace remnants. However, the OSL ages of the terrace remnants (samples 5 and 8) do not support this scenario, they indicate a Younger Dryas/early Holocene age for the remnants. The OSL age of the river dune on top of the terrace remnants (sample 9) however, does support this scenario. The dunes are dated at the end of the Younger Dryas. Implying that the dune was formed during the Younger Dryas, as expected. Stratigraphically this means that the underlying terrace should be older than the Younger Dryas, probably from the Bølling/Allerød.

Scenario 2

The second scenario (Younger Dryas-Holocene) assumes an incision at the cold-to-warm climatic transition at the start of the Holocene. An assumption is made concerning the Younger Dryas Meuse. It is assumed that the Meuse adapted an aggrading braided river style as a response to the cold period during the Younger Dryas. This caused the valley to fill with sediments. River dunes were formed on the stable east bank and on some of the more stable channel banks. At the transition to the Holocene the river starts meandering and incises into this Younger Dryas fill and removes most of it (figure 7.2). This incision scenario is comparable to the Pleniglacial-Bølling/Allerød incision, as both are a cold-to-warm transition The terrace remnant are supposedly what remains of the Younger Dryas floodplain.

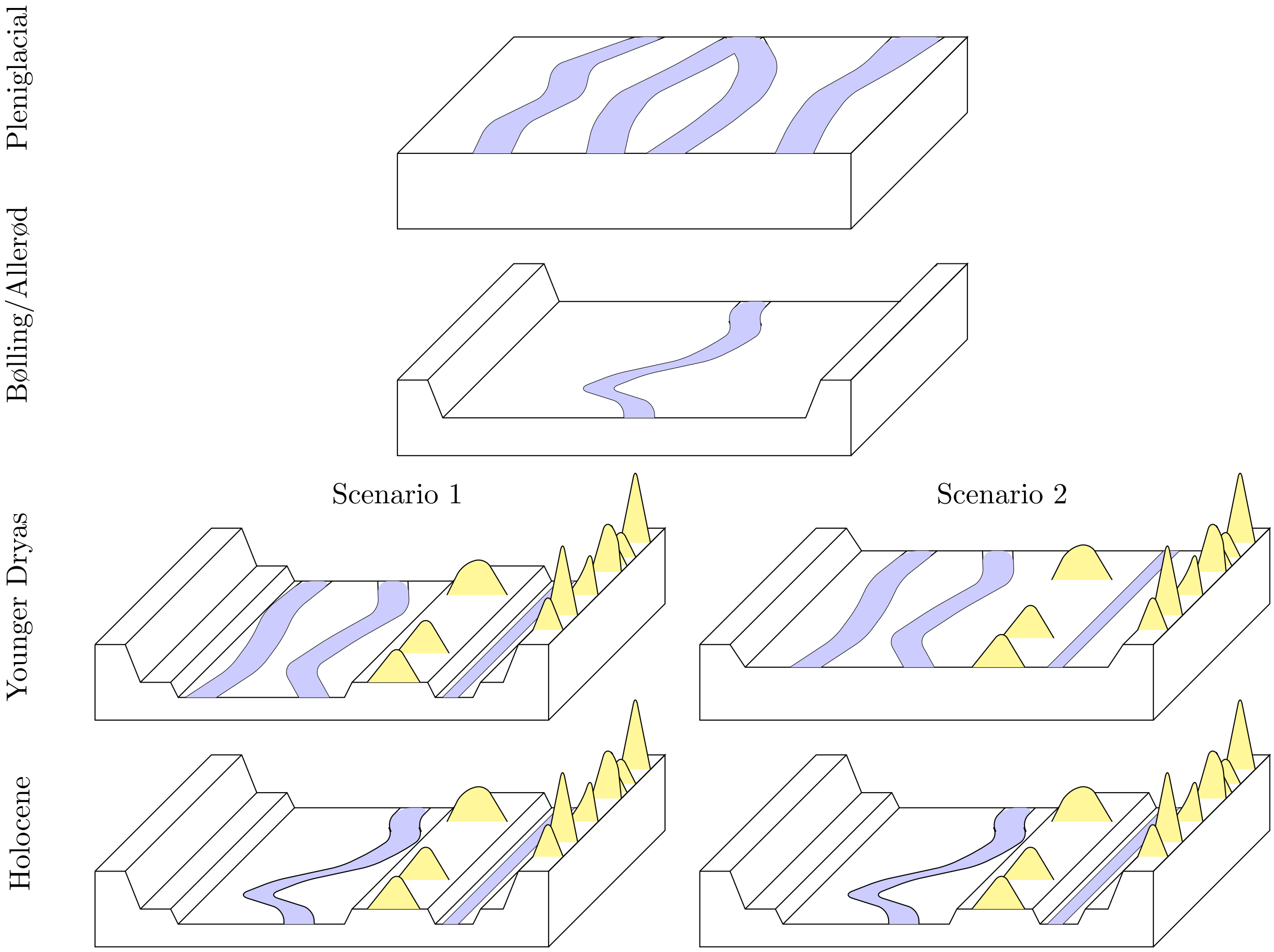

Figure 7.2: Schematic representation of the fluvial response based on the OSL ages. For the Younger Dryas/early Holocene two scenarios are given (see chapter 7.4.3).

Scenario 3

The third and final scenario is that at both climatic transitions a phase of incision occurred. There is no evidence to support or reject this possibility. The second Holocene incision could have made the Younger Dryas incision deeper.

River dunes

The river dunes were mainly formed during the Younger Dryas. These aeolian samples can tell something about the fluvial conditions during the Younger Dryas. These dunes consists of badly sorted sediments, for aeolian standards. This suggests that the sediments did not travel far and hence no sorting could take place. A logical source for the sediments would be the riverbed of the Meuse. A braided river often has a very low discharge, resulting in a dry riverbed with a lot of loose sediments that are vulnerable for aeolian transportation. When a channel is taken as the source of sediments, the lowest terrace level described at section 7.3.2 could be the source area for the dunes of sample 9, since the dominant wind direction was southwest, derived from the orientation of the parabolic dunes. In order for the dunes to form, some kind of stable micro-environment was necessary. Plants to capture the sediments are needed to form a dune. These plants could not survive in the active braided river plain of the Younger Dryas. It would have been more likely that these plants were growing on the slightly higher terraces. Consequently, the dunes formed on the slightly higher, probably older terraces.

7.4.4 Comparison of the theories

Two major phases of incision have been identified in this study. The first one on the cold-to-warm transition of the Pleniglacial to the Bølling and the second phase that has some uncertainty about its timing (section 7.4.3).

Both Huisink (1997) and Tebbens et al. (1999) agree on the first incision phase at the cold-to-warm incision. The only difference between the two is the response time of the Meuse and the rate of the incision. It is hard to chose a side based on the OSL ages obtained in this study.

Huisink (1997) and Tebbens et al. (1999) disagree on the second incision phase. Huisink (1997) describes a incision phase at the start of the Younger Dryas followed by aggradation during the remainder of the Younger Dryas and again an incision phase at the start of the Holocene. they do not agree on the incision at the warm-to-cold transition of the Younger Dryas. This shows the most resemblances with scenario 3 (section 7.4.3). Tebbens et al. (1999) see a return to an aggrading braided river system during the Younger Dryas. At the cold-to-warm transition they see a phase of incision. Their theory concerning the Younger Dryas shows the most resemblances with scenario 1 (section 7.4.3). Both studies (Huisink, 1997; Tebbens et al., 1999) see a different behavior of the Meuse during the Younger Dryas-early Holocene period. This study has three possible scenarios for the fluvial behavior of the Meuse during that period. Hence, it is not possible to draw a final conclusion concerning the second incision phase.

Then to answer the question whether or not to revise the theories concerning the fluvial response of the Meuse to climate change. Based on the new chronology made with the OSL ages in this research two incision phases can be recognized. The timing and cause of the incision phases however are different interpreted. The classic theory on fluvial climatic response with short phases of fluvial instability at both climatic transitions (Vandenberghe, 2008) seems to apply for the Late Glacial Meuse.

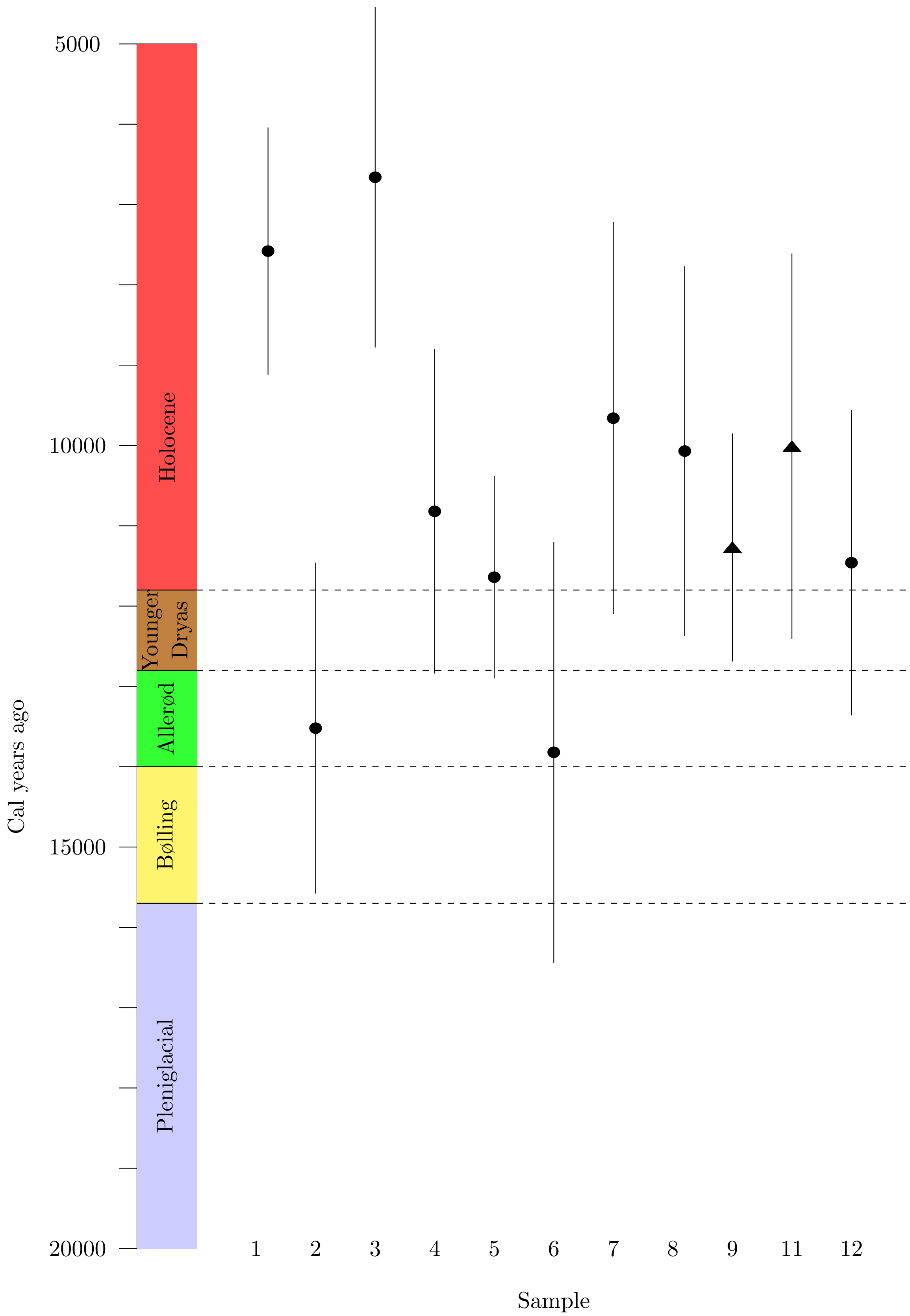

Figure 7.3: Time chart with the chronozones and the sample ages with their uncertainty. The fluvial samples are indicated with a circle and the aeolian samples are indicated by a triangle. Sample 10 is not included due to its young age.

Chapter 8

Conclusions

The Late Glacial/early Holocene Meuse sediments are generally well bleached. To deal with the partial bleaching that was present in several samples the minimum age model was used. For samples that did not show any signs of partial bleaching the minimum age model gave the same result as the central age model. Finally there was the difference in application of the MAM for the fluvial and aeolian samples. The aeolian samples have an unexpected higher overdispersion than the fluvial samples. Lowering the overdispersion as input for the aeolian MAM did not result in a better dose estimation. Resulting in the same usage of the MAM for both the fluvial and aeolian samples.

When comparing the OSL ages of the terraces, they are generally younger that expected. However, this can be explained with the post flood plain abandonment sedimentation. The resolution of the OSL dating was too coarse to statistically assign a terrace to a single chronozone. The Bølling and the Allerød interstadials can not be separated based on OSL ages obtained in this research.

The main objective was to create a new independent terrace chronology for the Late Glacial Meuse. This has been achieved, although there is still some uncertainty. Two incision phases are identified during the Late Glacial and early Holocene. The first incision as a response to the warming at the start of the Late Glacial and a second incision phase around the Younger Dryas stadial. The precise date of this second phase is still uncertain. More research would be required to gain more insight in this active period. The existing theories concerning the fluvial behavior of the Meuse to climate changes during the Late Glacial can not be rejected or accepted based on this study. More detail is needed concerning the Younger Dryas-early Holocene period.

Chapter 9

Recommendations

The data from this study indicate that the Younger Dryas-early Holocene was a very active period for the Meuse in northern Limburg. In order to be able to complete the chronology of the Late Glacial Meuse it is necessary to gain more detailed insight in the Younger Dryas-early Holocene period, because this study remained with some uncertainty about the timing of the incision at that period.

In order to be able to make a theory concerning the fluvial behavior of a river, it is recommended to sample terrace levels multiple times. There are two paths to do this.

In this research only one transect was made. To get a better view of the river response, it might be better to have multiple transects. In this way multiple terrace are sampled. When multiple terraces with the same elevation are sampled, the OSL age can be used to check whether they are formed in the same period and thus are one single terrace level. In this study each level was only sampled once or twice. Resulting in some difficulties when trying to place the terrace in a chronozone. When multiple age estimates are available of the same terrace level, it might be easier to place them in a chronozone. This would contribute to a better spatial resolution of the results.

The second way to improve the results by increasing the amount of samples is by taking multiple samples from one location/terrace, each sample from a different depth. In this way a separate chronosequence for each terrace can be made. In this way it would be possible to say more about the effect of post floodplain abandonment sedimentation on the ages of the terraces acquired in this research (figure 7.1). This method would be interesting to use on the terrace remnants. When this terrace level can be placed in a chronozone with high accuracy, it might answer the question of which scenario (see section 7.4.3) was most likely to occur during the Younger Dryas.

References

Berger, G. W., 1990. Effectiveness of natural zeroing of the thermoluminescence in sediments. Journal of Geophysical Research: Solid Earth (1978–2012) 95 (B8), 12375–12397.

Bohncke, S., 1993. Lateglacial environmental changes in the Netherlands: Spatial and temporal patterns: A contribution to the North Atlantic seaboard programme of IGCP-253, Termination of the Pleistocene. Quaternary Science Reviews 12 (8), 707–717.

Bøtter-Jensen, L., Andersen, C., Duller, G., Murray, A., 2003. Developments in radiation, stimulation and observation facilities in luminescence measurements. Radiation Measurements 37 (4), 535–541.

Bull, W. B., 1991. Geomorphic responses to climatic change. New York, NY (United States); Oxford University Press.

Colls, A., Stokes, S., Blum, M., Straffin, E., 2001. Age limits on the Late Quaternary evolution of the upper Loire River. Quaternary Science Reviews 20 (5), 743–750.

Cunningham, A., Wallinga, J., Minderhoud, P., 2011. Expectations of scatter in equivalent-dose distributions when using multi-grain aliquots for OSL dating. Geochronometria 38 (4), 424–431.

Cunningham, A. C., Wallinga, J., 2012. Realizing the potential of fluvial archives using robust OSL chronologies. Quaternary Geochronology 12, 98–106.

Duller, G., 2003. Distinguishing quartz and feldspar in single grain luminescence measurements. Radiation measurements 37 (2), 161–165.

Galbraith, R. F., Roberts, R. G., Laslett, G., Yoshida, H., Olley, J. M., 1999. Optical dating of single and multiple grains of quartz from jinmium rock shelter, northern australia: part i, experimental design and statistical models*. Archaeometry 41 (2), 339–364.

Gibbard, P., Rose, J., Bridgland, D., 1988. The history of the great Northwest European rivers during the past three million years [and discussion]. Philosophical Transactions of the Royal Society of London B: Biological Sciences 318 (1191), 559–602.

Grimm, E. C., Maher, L. J., Nelson, D. M., 2009. The magnitude of error in conventional bulk-sediment radiocarbon dates from central North America. Quaternary Research 72 (2), 301–308.

Hoek, W., 1997. Palaeography of Lateglacial vegetations: analysis in time and space. Ph.D. thesis, VU Amsterdam.

Hoek, W., 2000. Abiotic landscape and vegetation patterns in the Netherlands during the Weichselian Late Glacial. Netherlands Journal of Geosciences/Geologie en Mijnbouw 79 (4).

Hoek, W. Z., 2001. Vegetation response to the 14.7 and 11.5 ka cal. BP climate transitions: is vegetation lagging climate? Global and planetary change 30 (1), 103–115.

Houtgast, R., Van Balen, R., 2000. Neotectonics of the Roer Valley rift system, the Netherlands. Global and Planetary Change 27 (1), 131–146.

Huijzer, B., Vandenberghe, J., 1998. Climatic reconstruction of the Weichselian Pleniglacial in northwestern and central Europe. Journal of Quaternary Science 13 (5), 391–417.

Huisink, M., 1997. Late-glacial sedimentological and morphological changes in a lowland river in response to climatic change: the Maas, southern Netherlands. Journal of Quaternary Science 12 (3), 209–223.

Huisink, M., 1998. Tectonic versus climatic controls on the River Maas dynamics during the Lateglacial. Palaeohydrology and Environmental Change, 99–109.

Kasse, C., 1996. Younger Dryas cooling and fluvial response (Maas River, the Netherlands).

Kasse, C., 1997. Cold-Climate Aeolian Sand-Sheet Formation in North-Western Europe (c. 14–12.4 ka); a Response to Permafrost Degradation and Increased Aridity. Permafrost and Periglacial Processes 8 (3), 295–311.

Kasse, C., Vandenberghe, J., Van Huissteden, J., Bohncke, S., Bos, J., 2003. Sensitivity of Weichselian fluvial systems to climate change (Nochten mine, eastern Germany). Quaternary Science Reviews 22 (20), 2141–2156.

Mangerud, J., Andersen, S. T., Berglund, B. E., Donner, J. J., 1974. Quaternary stratigraphy of Norden, a proposal for terminology and classification. Boreas 3 (3), 109–126.

Miedema, R., Slager, S., Jongmans, A., Pape, T., 1983. Amount, characteristics and significance of clay illuviation features in late-Weichselian Meuse terraces. In: Soil micromorphology. International working meeting on soil micromorphology. 6. pp. 519–530.

Mol, J., Vandenberghe, J., Kasse, C., 2000. River response to variations of periglacial climate in mid-latitude Europe. Geomorphology 33 (3), 131–148.

Murray, A. S., Roberts, R. G., 1997. Determining the burial time of single grains of quartz using optically stimulated luminescence. Earth and Planetary Science Letters 152 (1), 163–180.

Murray, A. S., Wintle, A. G., 2000. Luminescence dating of quartz using an improved single-aliquot regenerative-dose protocol. Radiation measurements 32 (1), 57–73.

Olley, J. M., Roberts, R. G., Murray, A. S., 1997. Disequilibria in the uranium decay series in sedimentary deposits at Allen's Cave, Nullarbor Plain, Australia: implications for dose rate determinations. Radiation Measurements 27 (2), 433–443.

Preusser, F., Degering, D., Fuchs, M., Hilgers, A., Kadereit, A., Klasen, N., Krbetschek, M., Richter, D., Spencer, J. Q., 2008. Luminescence dating: basics, methods and applications. Quaternary Science Journal 57 (1-2), 95–149.

Rittenour, T. M., 2008. Luminescence dating of fluvial deposits: applications to geomorphic, palaeoseismic and archaeological research. Boreas 37 (4), 613–635.

Schumm, S., 1993. River response to baselevel change: implications for sequence stratigraphy. The Journal of Geology, 279–294.

Schumm, S. A., 1979. Geomorphic thresholds: the concept and its applications. Transactions of the Institute of British Geographers, 485–515.

Tebbens, L., Veldkamp, A., Westerhoff, W., Kroonenberg, S., 1999. Fluvial incision and channel downcutting as a response to Late-glacial and Early Holocene climate change: the lower reach of the River Meuse (Maas), the Netherlands. Journal of Quaternary Science 14 (1), 59–75.

Törnqvist, T. E., Dijk, G. J., 1993. Optimizing sampling strategy for radiocarbon dating of Holocene fluvial systems in a vertically aggrading setting. Boreas 22 (2), 129–145.

Van den Berg, 1996. Fluvial sequences of the Maas: a 10 Ma record of neotectonics and climate change at various time-scales. Ph.D. thesis, Landbouw Universiteit.

Vandenberghe, D., Derese, C., Kasse, C., 2013. Late Weichselian (fluvio-) aeolian sediments and

Holocene drift-sands of the classic type locality in Twente (E Netherlands): a high-resolution dating study using optically stimulated luminescence. Quaternary Science Reviews 68, 96–113.

Vandenberghe, J., 1993. Changing fluvial processes under changing periglacial conditions. Zeitschrift für Geomorphologie, Suppl. Bd 88, 17–28.

Vandenberghe, J., 1995. Timescales, climate and river development. Quaternary Science Reviews 14 (6), 631–638.

Vandenberghe, J., 2002. The relation between climate and river processes, landforms and deposits during the Quaternary. Quaternary International 91 (1), 17–23.

Vandenberghe, J., 2003. Climate forcing of fluvial system development: an evolution of ideas. Quaternary Science Reviews 22 (20), 2053–2060.

Vandenberghe, J., 2008. The fluvial cycle at cold–warm–cold transitions in lowland regions: a refinement of theory. Geomorphology 98 (3), 275–284.

Vandenberghe, J., 2014. River terraces as a response to climatic forcing: Formation processes, sedimentary characteristics and sites for human occupation. Quaternary International 370, 3–11.

Walker, M., 1995. Climatic changes in Europe during the last glacial/interglacial transition. Quaternary International 28, 63–76.

Walker, M., Bohncke, S., Coope, G., O'Connell, M., Usinger, H., Verbruggen, C., 1994. The Devensian/Weichselian Late-glacial in northwest Europe (Ireland, Britain, north Belgium, The Netherlands, northwest Germany). Journal of Quaternary Science 9 (2), 109–118.

Wallinga, J., 2002. Optically stimulated luminescence dating of fluvial deposits: a review. Boreas 31 (4), 303–322.

Woo, M.-K., Winter, T. C., 1993. The role of permafrost and seasonal frost in the hydrology of northern wetlands in North America. Journal of hydrology 141 (1), 5–31.

Appendix A

Table A.1: Information about the samples and sampling locations. The coordinates are in meters in the Dutch national grid (Rijksdriehoek) and the elevation is given in m +NAP.

Sample	Lab code	X	Y	Elevation	Method	date	Landuse
1	NCL-2615301	205684	390149	19.6	Auger	9-12-2015	Agriculture
2	NCL-2615302	206375	390829	18.7	Trench	9-12-2015	Forest
3	NCL-2615300	206569	391345	14.2	Trench	7-12-2015	Pasture
4	NCL-2615299	206643	391456	14.8	Trench	7-12-2015	Pasture
5	NCL-2615298	206798	391750	16.2	Trench	7-12-2015	Forest
6	NCL-2615297	206875	391891	15.4	Auger	7-12-2015	Agriculture
7	NCL-2615296	206943	391959	14.4	Auger	7-12-2015	Pasture
8	NCL-2615295	207078	392074	16.2	Trench	7-12-2015	Forest
9	NCL-2615294	207061	392280	19.1	Exposure	7-12-2015	Forest
10	NCL-2615303	207467	392713	14.3	Auger	9-12-2015	Pasture
11	NCL-2615305	208926	394433	28.7	Trench	9-12-2015	Forest
12	NCL-2615304	208784	394766	18.9	Trench	9-12-2015	Pasture

Appendix B

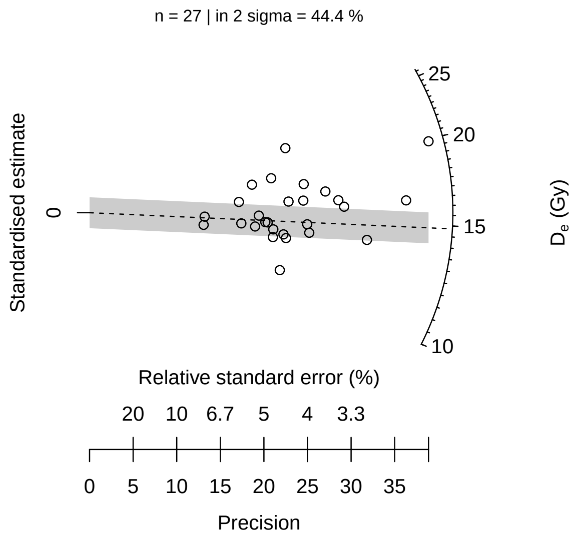

Figure B.1: Radial plot of sample 1 (NCL2615301)

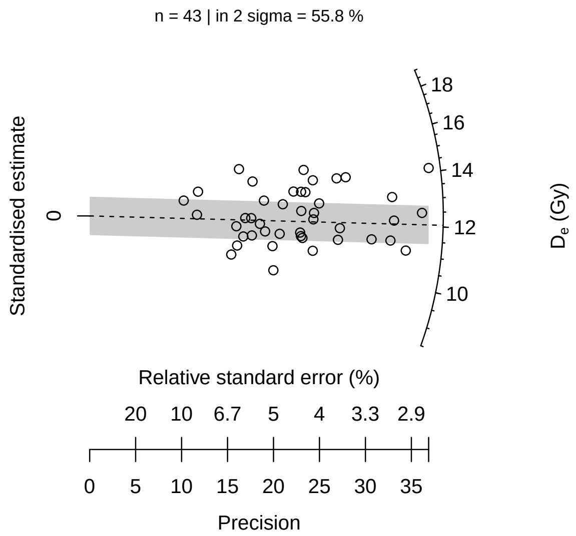

Figure B.2: Radial plot of sample 2 (NCL2615302)

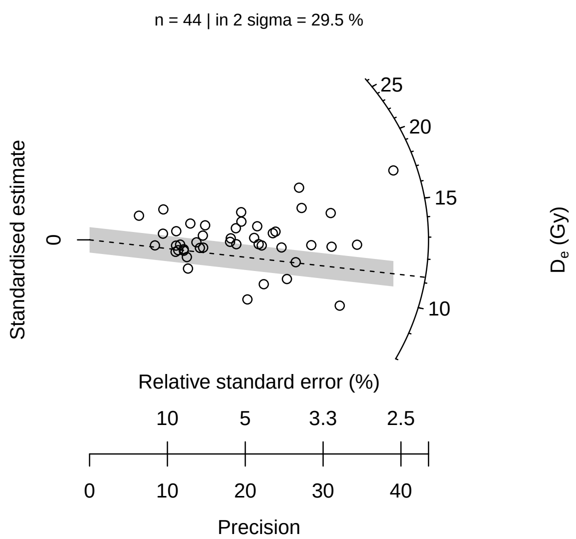

Figure B.3: Radial plot of sample 3 (NCL2615300)

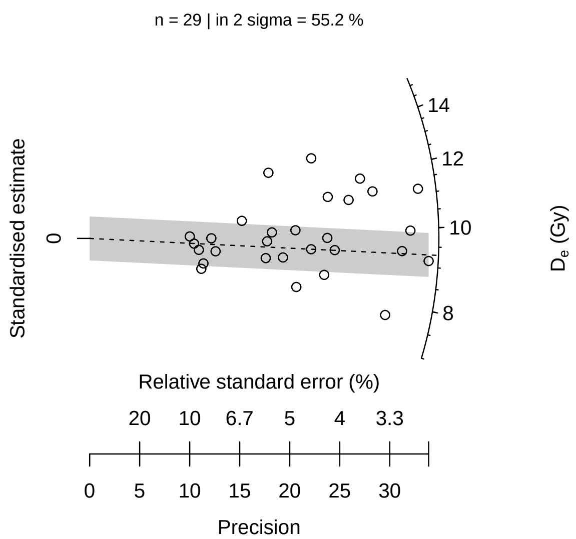

Figure B.4: Radial plot of sample 4 (NCL2615299)

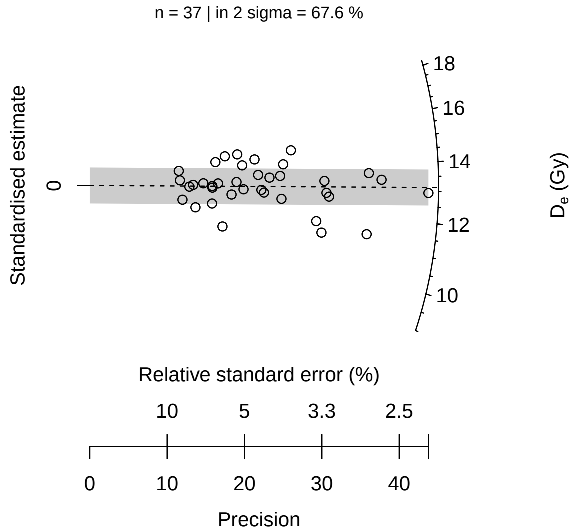

Figure B.5: Radial plot of sample 5 (NCL2615298)

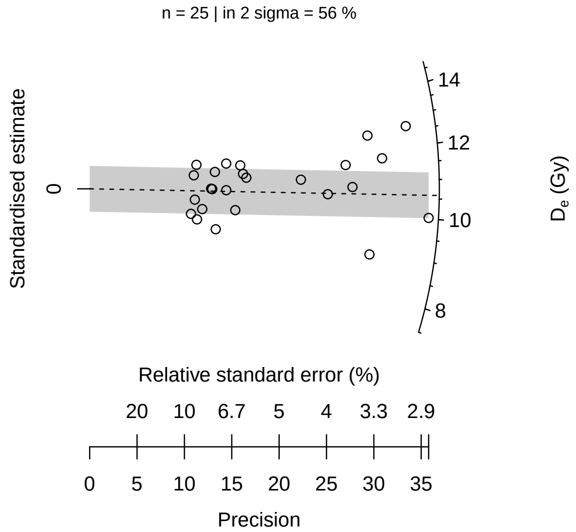

Figure B.6: Radial plot of sample 6 (NCL2615297)

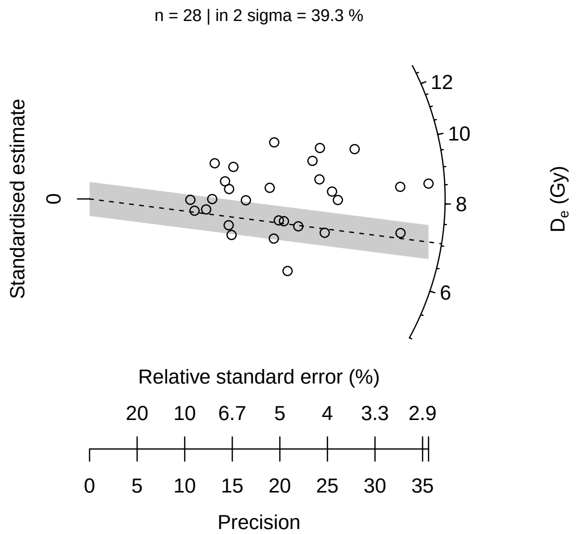

Figure B.7: Radial plot of sample 7 (NCL2615296)

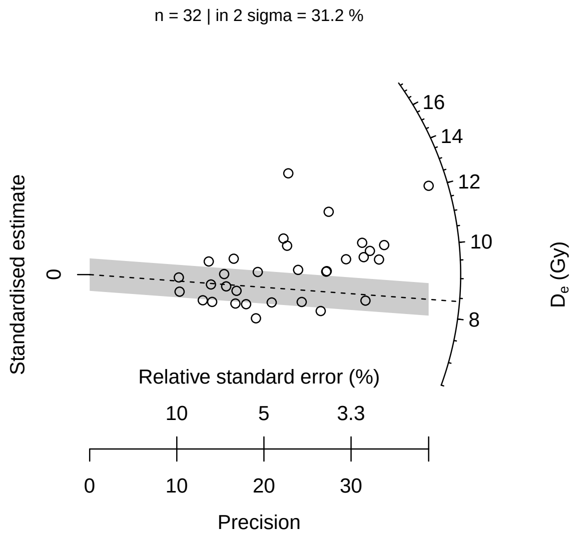

Figure B.8: Radial plot of sample 8 (NCL2615295)

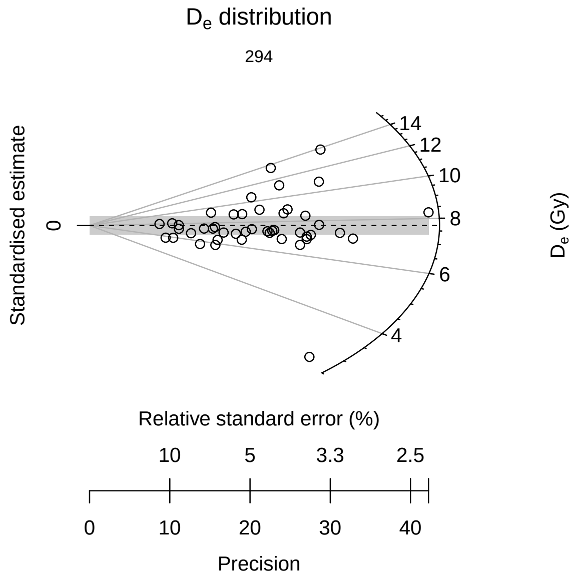

Figure B.9: Radial plot of sample 9 (NCL2615294)

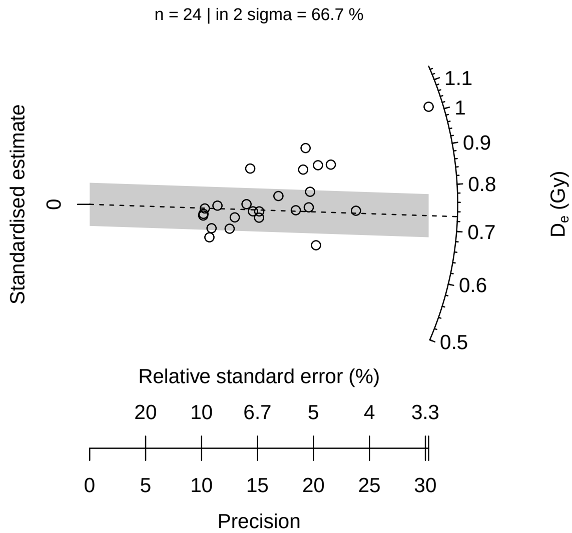

Figure B.10: Radial plot of sample 10 (NCL2615303)

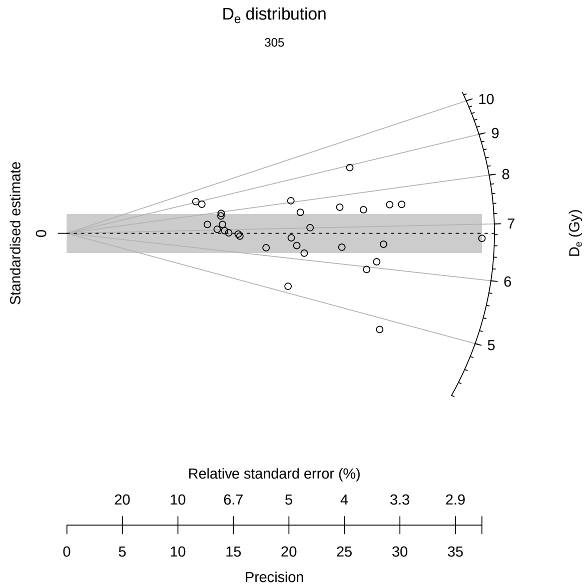

Figure B.11: Radial plot of sample 11 (NCL2615305)

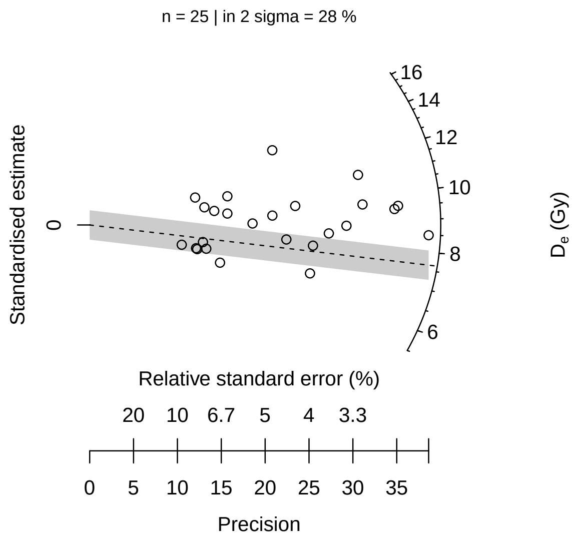

Figure B.12: Radial plot of sample 12 (NCL2615304)